ARCHER

Collaborative Project

Co-funded by the European Commission under the
Euratom Research and Training Programme on Nuclear Energy
within the Seventh Framework Programme

Grant Agreement Number: 269892
Start date: 01/02/2011Duration: 48 Months

www.archer-project.eu

Deliverable D42.12: Compilation of reference mechanical and micro-structural data for 800H and weldments

M. Kolluri (NRG)

BIO-PROTECT – Contract Number: 269892
Advanced High-Temperature Reactors for Cogeneration of Heat and Electricity R&D

Document title	Deliverable D42.12: Compilation of reference mechanical and micro-structural data for 800H and weldments
Author(s)	M Kolluri (NRG)
Number of pages	71
Document type	Deliverable
Work Package	WP42
Document number	D-42-12:
Issued by	D Buckthorpe (AMEC)
Date of completion	31/12./2013…
Dissemination level	Confidential, only for consortium members (including the Commission Services)

Summary

This document contains the results from the ARCHER SP4 Workpackage 2 activity on the development of reference mechanical and micro-structural data for 800H and weldments. The scope of work is focussed on mechanical tests and microscopy studies.

The report provides results from tests perfomed at NRG on Alloy 800H parent plate and weld. The scope covers tensile tests at room temperature, 700^{o}C and 800^{o}C in air to address monotonic behaviour; low cycle fatigue tests (with and without tensile hold times at four different strain ranges) on parent plate material to investigate cyclic behaviour and influence of hold time on strain-life behaviour; and their reference microstructural investigations.

The tensile results show a significant reduction in strength properties between 700 and 800oC. Fatigue life is substantially affected by tensile hold time with the maximum reduction occuring at the lowest starin range. Microstructural studies on the parent plate and weld show a high concentration of small spheroidal inclusions (mainly Nb-Ti) in the weld consistent with an effective shielding of the weld pool (from oxygen) during the GTAW process.

For the tensile results a good agreement is seen with recent published results from the ASME LLC on the development of Allowable Stresses in ASME Section III NH for Alloy 800H and which indicates that in all cases the weld strength is better than that of the parent plate.

This report provides the status of the investigative work on the mechanical and microstructural investigations within WP42 Task 2 for Alloy 800H up to the 3rd year of the ARCHER Progamme.

Approval

Rev.	Date	First author	SP leader	Project Coordinator
0	month/year 31/12/13	M Kolluri (NRG)	D Buckthorpe; AMEC	S Knol;NRG

Distribution list

Name	Organisation	Comments
All beneficiaries	ARCHER	Through internet workspace
WP4 Participants	ARCHER	Through internet workspace

Table of contents

1 Introduction ... 4
2 Results from Tensile & Fatigue tests and Microscopy at NRG (Attachment A) ... 4
3 Comparison with Allowable Stresses in ASME Section III NH for Alloy 800H ... 4
4 Conclusions ... 13
5 References ... 13
Appendix A: NRG Report on Reference Characterisation of Alloy 800H ... 14

1 Introduction

This covers the investigation of 'Alloy 800 H' material and weldments. The task is the part of the work package 4.2 (WP42) of the large European project ARCHER, which is mainly targeted at extending the state-of-the-art European technology basis for (Very) High Temperature Rectors, (V)HTR. The objective of the work is to characterize the reference mechanical properties (creep/creep-fatigue interactions) of the Alloy 800 H (base and weld material) at temperatures ranging from RT to 750^{O}C and to carry out the micro-structural studies on the base and weld materials. The main activities are associated with (i) material procurement, (ii) sample fabrication, (iii) microscopy, (iv) mechanical testing and finally (v) reporting of the total work. In view of the level of funding, the focus has been kept on studying the creep-fatigue interactions with low cycle fatigue (LCF) tests with hold time (at peak stresses) for only one chosen temperature in air/vacuum and the microscopic investigations using OM, SEM and/TEM. Preliminary microscopic studies have also been performed on the weld Alloy 800H material using OM and SEM. No irradiation experiments will be performed in this part of project. The original work scope included an additional contribution from JRC but due to resource reductions this contribution was no longer available and the contribution form NRG has been used for this work. A summary of the results at NRG is given in section 2 and contained in Appendix A. Section 3 summarises a comparison of available tensile results against recent published results from the ASME LLC on the development of Allowable Stresses in ASME Section III NH for Alloy 800H [Ref 1].

2 Results from Tensile & Fatigue tests and Microscopy at NRG (Attachment A)

The objective of 'this work is to characterize the reference mechanical properties (tensile and creep/creep-fatigue interactions) of the alloy 800H base and weld material at temperatures ranging from temperatures of RT to 800°C and to carry out micro-structural studies on the materials. The primary focus was to study the base material properties and according to an agreement reached between the project partners, the testing of weld material depends upon the availability of leftover material and budget. Following discussion at the first ARCHER progress meeting in Julich, the following was agreed:

- Perform tensile testing at 3 different temperatures in air environment.
- Perform low cycle fatigue (LCF) tests with and without hold time at the peak stresses (for creep-fatigue interaction study); to be performed at one single temperature in air environment and at 4 different strain ranges.
- Perform limited scale microscopic studies using optical microscopy (OM), scanning electron microscopy (SEM) and transmission electron microscopy (TEM).
- Compile the results of the tensile and fatigue/creep-fatigue interaction tests, including the results from the micro-structural investigation into a report.

The results of the investigations are given in Attachment A

The findings are compared with available ASME information as discussed in section 3 below.

3 Comparison with Allowable Stresses in ASME Section III NH for Alloy 800H

3.1 Tensile & Yield stress results

Tensile tests on Alloy 800H base and weld materials have been performed at RT, 700°C and 800°C. In both the base and weld materials, a considerable decrease of the strength properties (YS and UTS) has been observed with increasing the temperature, particularly with the reduction in UTS from 700°C to 800°C. Below a comparison of the results is made against the available ASME results given in Ref [1]. The ASME results have been extracted from Part II of Ref [1] and are shown below in Figures 1a) and 1b). The corresponding NRG test results are shown in Figure 1c).

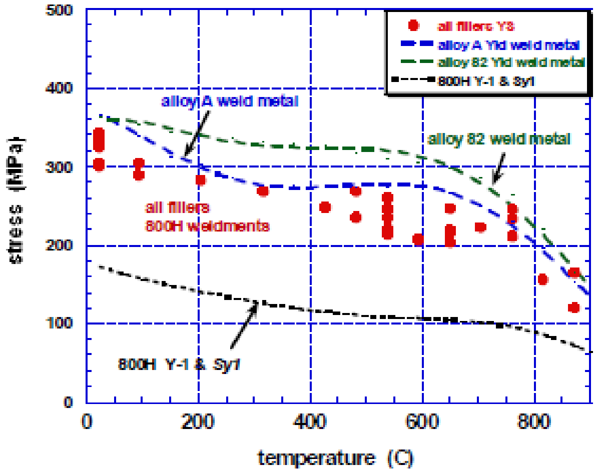

Figure 1 (a) ASME results: Comparison of weldment yield strength with base metal Alloy 800H

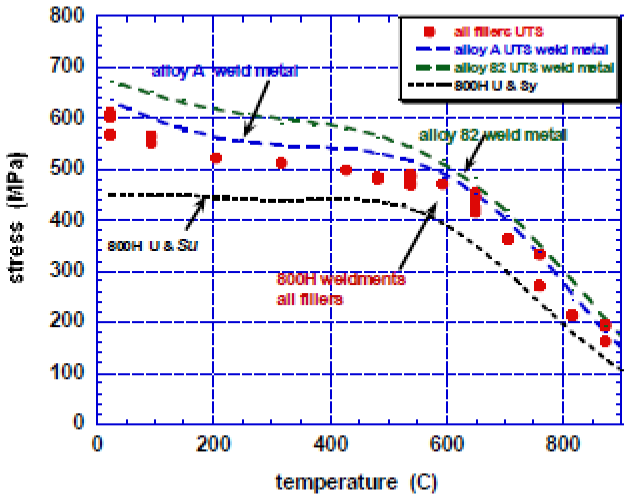

Figure 1 (b) ASME results: Comparison of weldment tensile strength with base metal Alloy 800H

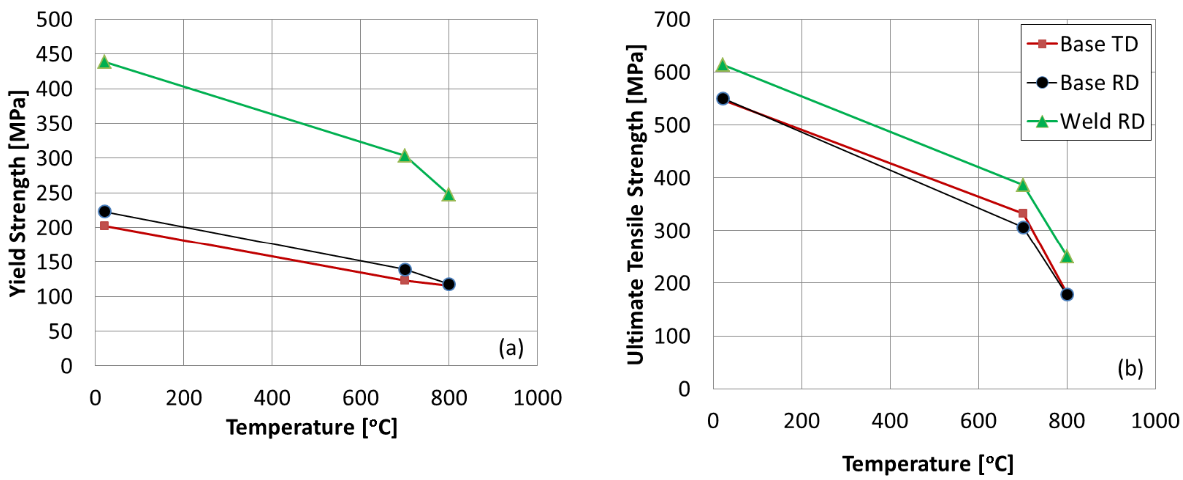

Figure 1 (c) NRG results: Comparison of tensile and Yield strength Of base metal Alloy 800H

The results show that the measured sharp fall off in tensile strength between 700 and 800°C is consistent with the results presented by ASME. The weldment strength is greater than that of the parent material and again consistent with the ASME values. An analysis of the tensile and yield data used within the ASME Section NH is given in Ref [2] using a trend curve based on the ratio of the elevated temperature strength to the room temperature strength. The resulting allowable stress values for the material over the range RT to 900°C are given in Ref [2] and compared with other alloys used in ASME NH in Ref [3]. The recommended allowable stress intensity values for Alloy 800H up to 900°C from Ref [2] are shown below in Table 1.

The current values for Y-1 and U in ASME Section II, Part D should be retained to their current temperature limits (1000°F or 525°C).

The value for Y-1 at 1000°F (525°C) Section II, Part D should replace the newly calculated Sy1 values in Table I-14.5 until the newly calculated SY1 values fall below the Y-1 value at 1000°F (525°C).

The Sm values are based on the lower of 90% Y-1 and U/3 from ASME II-D Table Y-1 and Table U for temperatures to 1000°F and 525°C. Above these temperatures, values based on 90%SY1 and SU/3 from the below table are recommended:

The following values to 900°C then apply:

Temp ℃	R_Y	S_yR_y MPa	S_{y1} MPa		R_T	$1.1S_TR_T$ MPa	S_U MPa		$\boldsymbol{S_m}$ MPa
425									104
450									102
475									101
500									99.0
525									97.2
550	**0.651**	112	108		**0.816**	402	402		97.2
575	**0.646**	111	108		**0.793**	391	391		97.2
600	**0.639**	110	108		**0.766**	378	378		97.2
625	**0.631**	109	108		**0.735**	362	362		97.2
650	**0.621**	107	107		**0.700**	345	345		96.3
675	**0.608**	105	105		**0.661**	326	326		94.5
700	**0.593**	102	102		**0.618**	305	305		91.8
725	**0.575**	99.1	99.1		**0.572**	282	282		89.2
750	**0.554**	95.6	95.6		**0.524**	258	258		86.0
775	**0.531**	91.5	91.5		**0.473**	233	233		77.8
800	**0.504**	86.9	86.9		**0.422**	208	208		69.3
825	**0.475**	81.8	81.8		**0.369**	182	182		60.9
850	**0.442**	76.3	76.3		**0.318**	157	157		52.2
875	**0.408**	70.3	70.3		**0.268**	132	132		44.0
900	**0.371**	64.0	64.0		**0.221**	109	109		36.4

Table 1 ASME Recommended Allowable Stress Intensity Values (S_Y, S_U, S_m) for Alloy 800H: (425 to 900°C), from Ref [2]

3.2 Values for S_t

Within the ASME Code the short-time values for S_t are controlled by the value of the hot tensile curve at 1% strain over much of the temperature range from 425 to 725°C. Most of the values at intermediate temperatures and the longer times and higher temperature values are controlled by the time to initiate tertiary creep. Although no specific tests have been performed within this task to compare against these ASME S_t values, the recommended ASME S_t values have been reproduced here for information to provide a comparison with the values used for the design of the compact and full size IHX investigations in WP43. Recommended ASME values for S_t from Ref [2] are shown diagrammatically in Figure 2 and in tabular form in Table 2.

Table I-14.4C

S_t - Allowable Stress Intensity Values, MPa, Ni-Fe-Cr (Alloy 800H)

SI Units

Temp., °C	1 hr	3 hr	10 hr	30 hr	100 hr	300 hr	1,000 hr	3,000 hr	10,000 hr	30,000 hr	100,000 hr	300,000 hr	500,000 hr
425	164	164	164	164	164	164	164	164	164	164	164	164	164
450	162	162	162	162	162	162	162	162	162	162	162	162	162
475	160	160	160	160	160	160	160	160	160	160	156	137	129
500	157	157	157	157	157	157	157	157	157	150	129	113	106
525	155	155	155	155	155	155	155	155	143	124	107	92.2	86.2
550	155	155	155	155	155	155	155	140	119	103	87.6	75.3	70.1
575	155	155	155	155	155	155	136	117	99.4	85.2	71.8	61.2	56.8
600	155	155	155	155	155	136	115	98.2	82.5	70.2	58.6	49.6	45.8
625	155	155	155	155	135	115	96.4	81.8	68.2	57.5	47.6	40.0	36.8
650	154	154	154	137	114	97.0	80.7	68.0	56.1	47.0	38.6	32.1	29.4
675	151	151	138	117	97.0	81.6	67.3	56.3	46.1	38.3	31.1	25.6	23.4
700	148	143	119	99.6	82.0	68.5	56.0	46.4	37.7	31.0	24.9	20.3	18.5
725	144	123	101	89.6	69.1	57.3	46.4	38.2	30.7	25.0	19.9	16.1	14.5
750	117	106	86.6	71.7	58.1	47.7	38.3	31.2	24.9	20.1	15.8	12.6	11.3
775	110	91.1	73.8	60.6	48.7	39.7	31.6	25.5	20.0	16.0	12.4	9.82	8.78
800	95.0	78.1	62.7	51.1	40.7	32.9	25.9	20.7	16.1	12.7	9.75	7.60	6.75
825	81.8	66.7	53.1	43.0	33.9	27.1	21.1	16.7	12.8	10.0	7.58	5.83	5.14
850	70.3	56.9	44.9	36.0	28.1	22.3	17.2	13.4	10.2	7.86	5.85	4.43	
875	60.1	48.4	37.9	30.1	23.2	18.2	13.9	10.7	8.04	6.11	4.48		
900	51.3	41.1	31.8	25.0	19.1	14.9	11.2	8.54	6.29	4.72			

Table 2 ASME Recommended Allowable Stress Intensity Values (S_t) for Alloy 800H: (425 to 900°C), from Ref [2]

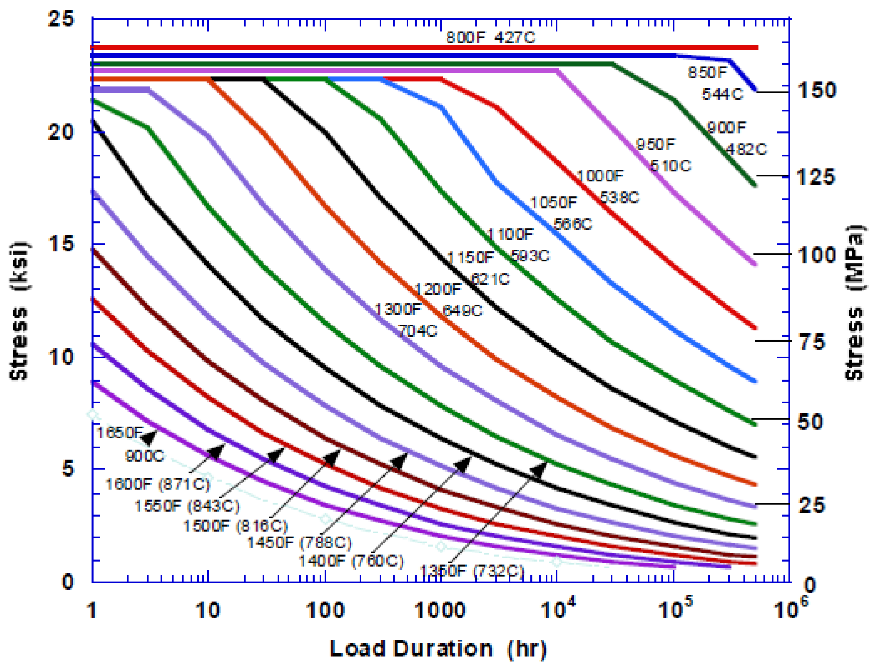

Figure 2 ASME Recommended values for St verses Temperature for Alloy 800H (taken from Ref [2])

3.3 Values for S_{mt}

The low temperature short time values of S_{mt} are controlled by the value of S_m. For Alloy 800H, most of the remaining values are controlled by the stress corresponding to the time to initiate tertiary creep. The recommended values within ASME for Alloy 800H are given in Ref [2]. Although no specific tests have been performed within this task to compare against these ASME S_{mt} values, the recommended ASME S_{mt} values have been reproduced here for information to provide a comparison with the values used for the design of the compact and full size IHX investigations in WP43. Recommended ASME values for S_{mt} from Ref [2] are shown diagrammatically in Figure 3 and in tabular form in Table 3.

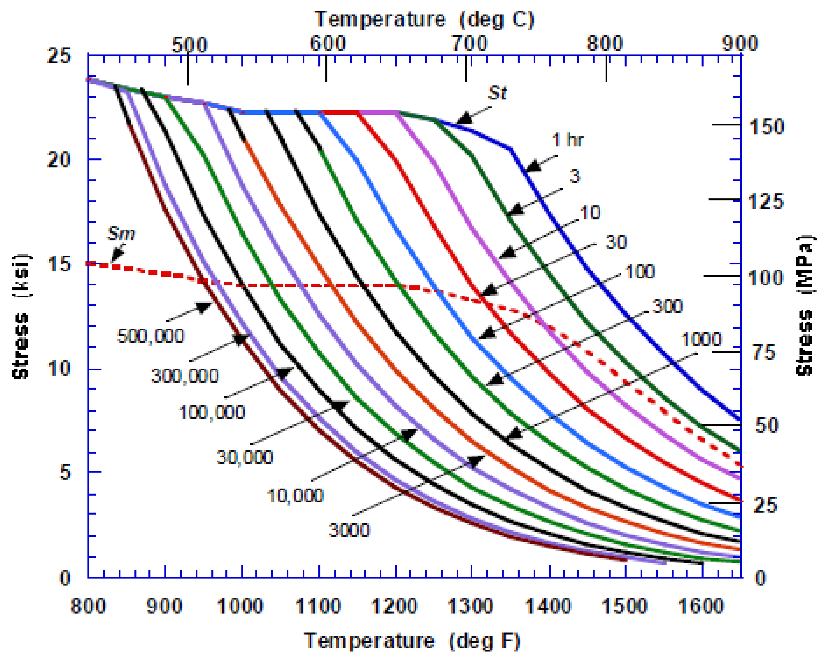

Figure 3 ASME Recommended values for Smt verses Temperature for Alloy 800H (taken from Ref [2])

S_{mt} - Allowable Stress Intensity Values, MPa, Ni-Fe-Cr (Alloy 800H)

SI Units

Temp., °C	1 hr	3 hr	10 hr	30 hr	100 hr	300 hr	1,000 hr	3,000 hr	10,000 hr	30,000 hr	100,000 hr	300,000 hr	500,000 hr
425	104	104	104	104	104	104	104	104	104	104	104	104	104
450	102	102	102	102	102	102	102	102	102	102	102	102	102
475	101	101	101	101	101	101	101	101	101	101	101	101	101
500	99.0	99.0	99.0	99.0	99.0	99.0	99.0	99.0	99.0	99.0	99.0	99.0	99.0
525	97.2	97.2	97.2	97.2	97.2	97.2	97.2	97.2	97.2	97.2	97.2	92.2	86.2
550	97.2	97.2	97.2	97.2	97.2	97.2	97.2	97.2	97.2	97.2	87.6	75.3	70.1
575	97.2	97.2	97.2	97.2	97.2	97.2	97.2	97.2	97.2	85.2	71.8	61.2	56.8
600	97.2	97.2	97.2	97.2	97.2	97.2	97.2	98.2	82.5	70.2	58.6	49.6	45.8
625	97.2	97.2	97.2	97.2	97.2	97.2	96.4	81.8	68.2	57.5	47.6	40.0	36.8
650	96.3	96.3	96.3	96.3	96.3	96.3	80.7	68.0	56.1	47.0	38.6	32.1	29.4
675	94.5	94.5	94.5	94.5	94.5	81.2	67.3	56.3	46.1	38.3	31.1	25.6	23.4
700	91.8	91.8	91.8	99.6	81.6	68.5	56.0	46.4	37.7	31.0	24.9	20.3	18.5
725	89.2	89.2	89.2	89.2	69.1	57.3	46.4	38.2	30.7	25.0	19.9	16.1	14.5
750	86.0	86.0	86.0	71.7	58.1	47.7	38.3	31.2	24.9	20.1	15.8	12.6	11.3
775	77.8	77.8	73.8	60.6	48.7	39.7	31.6	25.5	20.0	16.0	12,4	9.82	8.78
800	69.3	69.3	62.7	51.1	40.7	32.9	25.9	20.7	16.1	12.7	9.75	7.60	6.75
825	60.9	60.9	53.1	43.0	33.9	27.1	21.1	16.7	12.8	10.0	7.58	5.83	5.14
850	52.2	52.2	44.9	36.0	28.1	22.3	17.2	13.4	10.2	7.86	5.85	4.43	3.88
875	44.0	44.0	37.9	30.1	23.2	18.2	13.9	10.7	8.04	6.11	4.48		
900	36.4	36.4	31.8	25.0	19.1	14.9	11.2	8.5	6.29	4.72			

Table 3 ASME Recommended Allowable Stress Intensity Values (S_{mt},) for Alloy 800H: (425 to 900°C), from Ref [2]

3.4 Values for S_r

Minimum recommended ASME values for stress to rupture for Alloy 800H are also listed in Ref [2] for temperatures from 425 to 900°C. Again no specific tests have been performed by NRG within this task of ARCHER for comparison. The recommended values provided by ASME have been reproduced below for information and for comparison with the values used for the design of the compact and full size IHX investigations in WP43. Recommended ASME values for S_r from Ref [2] are shown diagrammatically in Figure 3 and in tabular form in Table 3.

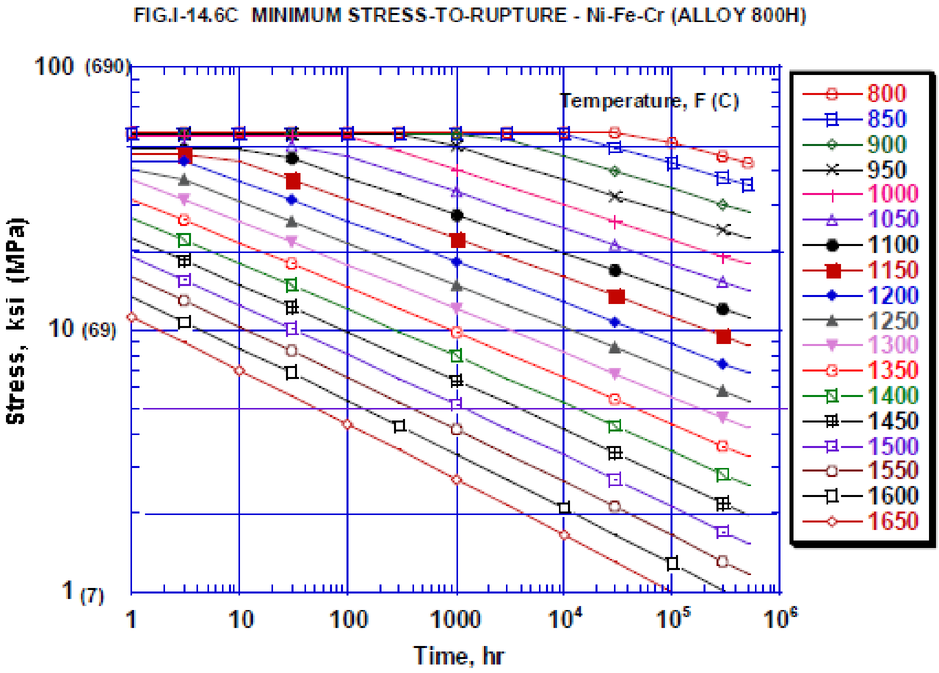

Figure 3 ASME Recommended values for Sr verses Temperature for Alloy 800H (taken from Ref [2])

The extension of ASME III-NH to higher temperatures and longer times is also dependent on resolving issues related to weldment performance. Weld Strength Reduction Factors (SRF) currently provided in ASME III-NH for alloy 800H are not adequately supported by the available database for temperatures in excess of 730℃ Ref [3]. No strength tests were performed by NRG within Task 2 of WP42. Within ARCHER some testing of Alloy 800H welds and weldments are planned to assess representative weld factors for application to the Plate type IHX as part of the work of WP43. Results from these tests will be used to check against the weldment factors used in ASME III NH when these are available.

EXPECTED MINIMUM STRESS-TO-RUPTURE VALUES, MPa, Ni-Fe-Cr (ALLOY 800H) (CONT'D)

SI Units

Temp. °C	1 hr	3 hr	10 hr	30 hr	100 hr	300 hr	1,000 hr	3,000 hr	10,000 hr	30,000 hr	100,000 hr	300,000 hr	500,000 hr
425	387	387	387	387	387	387	387	387	387	387	374	330	312
450	385	385	385	385	385	385	385	385	385	354	307	270	254
475	384	384	384	384	384	384	384	384	333	292	252	220	207
500	382	382	382	282	382	382	369	321	276	241	207	180	168
525	379	379	379	379	379	361	309	268	229	198	169	146	137
550	352	352	352	352	351	303	258	223	189	163	138	119	111
575	342	342	342	342	297	255	216	185	156	134	113	96	90
600	331	331	331	297	250	214	180	154	129	110	92	78	72
625	317	317	296	252	211	180	150	127	106	90	75	63	58
650	302	302	252	214	178	150	125	105	87	73	61	51	47
675	285	259	215	181	150	126	104	87	72	60	49	41	38
700	264	221	183	153	126	105	86	72	59	49	40	33	30
725	227	189	155	129	106	88	71	59	48	40	32	26	24
750	195	162	132	109	89	73	59	49	39	32	26	21	19
775	167	138	112	92	74	61	49	40	32	26	21	17	15
800	143	118	95	77	62	51	40	33	26	21	17	13	12
825	123	100	80	65	52	42	33	27	21	17	13	11	9.7
850	105	85	68	55	43	35	27	22	17	14	11	8.5	7.6
875	90	72	57	46	36	29	23	18	14	11	8.5	6.7	6.0
900	77	61	48	38	30	24	18	15	11	8.9	6.8	5.3	4.7

Table 3 ASME Recommended Allowable Stress to Rupture Values (S_r,) for Alloy 800H: (425 to 900^{o}C), from Ref [2]

3.5 Cyclic testing and Fatigue results

The cyclic stress-strain behaviour of Alloy 800H specimens (0.6% total strain range) has been obtained with and without hold time (Appendix A). The hold time has been applied in tension only. For presentation of the cyclic stress-strain behaviour, only 4 cycles (i.e. cycle number 2, the cycle in which the saturation stress has been reached, and the cycles in which the peak tensile stresses ( ) have dropped by 25% (N25) and the 50% (N50) cycle have been illustrated. The conclusion from the NRG tests is that a considerable strain softening can be seen in all the tests after an initial hardening followed by a plateau regime. In the case of hold time tests, a clear drop in the maximum stress is observed during the hold period at the maximum tensile strain () indicating a clear stress-relaxation behaviour for the material at 800°C. This behaviour leads to a considerable reduction in low cycle fatigue life of this material in hold time tests at all 4 strain ranges at 800°C (Figure 4.1).

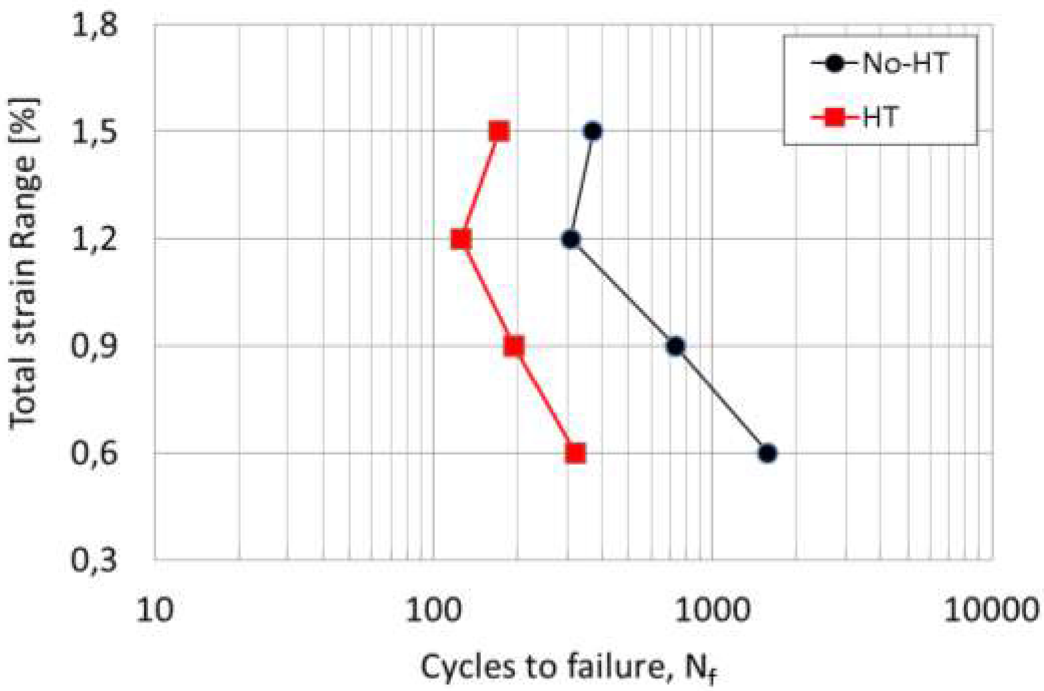

Figure 4.1 Comparison of the strain-life curves of the no-HT and HT tests at 800oC.

Tests performed by NRG are for strain ranges of 0.6 % or greater. The data base at Petten includes continuous cycle data with limited information on stabilised hysteresis loops and stress ranges. Information on continuous cycling behaviour and creep-fatigue behaviour are also available in the ASME III-NH Code with information up to 850°C. Ref [3] refers to poor hardening characteristics of solid-solution nickel based alloys above 800°C that can contribute to instability in fatigue specimens when tested and that for the HTR fatigue information at low strain ranges and long times will be the most appropriate with regard to operation behaviour.

3.6 Other Issues

Other issues to note from Ref [3] that may need clarification are effects of stabilisation heat treatment, strain rate effects on strength and ductility, diffusion creep and multi-axial creep rupture. Several austenitic alloys, including alloy 800H and Alloy 617 are susceptible to "relaxation cracking" in the service temperature range of 575 to 700°C (750°C for the case of alloy 617). Failures have been observed in the process industry and a second "stabilization heat treatment" at 980°C after the solution heat treatment is recommended to avoid relaxation cracking in alloy 800H. If introduced in ASME III-NH, the stabilization heat treatment could have an effect on the yield and ultimate tensile strengths. Ref [3] therefore recommends that the extent of the effect should be established from a few tensile tests over the range of temperatures covered by S_U and S_{y1}.

4 Conclusions

Results from tests perfomed at NRG on Alloy 800H parent plate and weld are presented. The scope of the tests includes tensile tests at room temperature, 700°C and 800°C in air to address monotonic behaviour; low cycle fatigue tests (with and without tensile hold times at four different strain ranges) on parent plate material to investigate cyclic behaviour and influence of hold time on strain-life behaviour; and their reference microstructural investigations.

The tensile results show a significant reduction in strength properties between 700 and 800°C. Fatigue life is substantially affected by tensile hold time with the maximum reduction occuring at the lowest starin range. Microstructural studies on the parent plate and weld show a high concentration of small spheroidal inclusions (mainly Nb-Ti) in the weld consistent with an effective shielding of the weld pool (from oxygen) during the GTAW process.

For the tensile results a good agreement is seen with recent published results from the ASME LLC on the development of Allowable Stresses in ASME Section III NH for Alloy 800H and which indicates that in all cases the weld strength is better than that of the parent plate.

Design data recently derived for Alloy 800H for application in the ASME Code are presented for the allowables stress values S_m, S_t, S_{mt}, S_r up to 900°C. The NRG results for fatigue tests with tensile holds are presented and show a considerable strain softening and stress-relaxation behaviour for the material above 800°C.

5 References

[1] Verification of Allowable Stresses in ASME Section III Subsection NH for ALLOY 800H, R. W. Swindeman, et. Al, STP-NU-020, ASME Standards Technology LLC, 2009

[2] Extend Allowable Stress values for ALLOY 800H, R. W. Swindeman, et. Al, STP-NU-035, ASME Standards Technology LLC, 2012

[3] New Materials for ASME Subsection NH, R. K Suzuki & T Asayama, JAEA, STP-NU-042, ASME Standards Technology LLC, 2011

Appendix A: NRG Report on Reference Characterisation of Alloy 800H

NRG report on reference characterization of "Archer Alloy 800H"

Confidential

Under the contract of Archer

rev. no.	date	description
A		1st draft
B		Final after internal review
C		Final

author(s):	Kolluri, N.V.V.R. (Murthy) K. N.V.V. Ramana Murty 07-03-2014	reviewed:	T.O. van Staveren 7-3-'14
name:	119847revC Report on Archer Alloy 800H_final.docx	approved:	J.A. Vreeling 7-3-2014
referencenr.:	NRG-22907/14.119847revC		
60 pages	05/03/2014		

© NRG 2014

Subject to agreement with the client, the information contained in this report may not be disclosed to any third party and NRG is not liable for any damage arising out of the use of such information.

Contents

Summary		5
1	Project description	7
1.1	Background	7
1.2	Scope of the Alloy 800H project	7
1.3	Activities planned	8
2	Experimental	9
2.1	Material	9
2.2	Mechanical characterization	9
2.2.1	Tensile tests	9
2.2.2	Low-cycle fatigue (LCF) test	10
2.2.3	Test matrix	11
2.3	Microscopic examination	12
3	Results	13
3.1	Tensile tests	13
3.2	Low cycle fatigue (LCF) tests	16
3.2.1	Cyclic stress-strain behavior	16
3.2.2	Evolution of the maximum cyclic tensile and compressive stresses and influence of the hold time	17
3.3	Microstructure of Alloy 800H base ans weld materials	20
3.3.1	Microstructure of Alloy 800H base material	20
3.3.2	Microstructure of Alloy 800H weld material	23
3.3.3	Hardness Alloy 800H base and weld material	25
4	Discussion	27
4.1	Tensile properties	27
4.2	Creep-fatigue properties	28
4.2.1	Effect of the hold time on the fatigie life	28
5	Conclusions	29
6	Recommendations for the future work	30
References	31	

List of tables 33

List of figures 33

Appendix A 35

A.1 Material data sheet: Alloy 800H base material 35

A.2 Material data sheet: Alloy 800H weld material 37

Appendix B 42

B.1 Single specimen data of all the tensile tests 42

B.2 Single specimen data of all LCF tests 43

Appendix C 44

C.1 EDS results precipitate analyses of Base Material 44

C.2 EDS results of weld material 53

Summary

This report summarize the results from mechanical testing and preliminary microscopy study of Archer Alloy 800H.

This report is organized as follows. First, a brief description about the project is given including the scope and various activities agreed in this project. Then, the details about specimen preparation, test matrix and experiments are given. Finally, all the mechanical testing and microscopy results are summarized and conclusions are drawn with some recommendations for future work.

1 Project description

1.1 Background

ARCHER is a large European project, launched mainly with a target of extending the state-of-the-art European technology basis for (Very) High Temperature Rectors, (V)HTR. Total project is divided into 6 sub projects (SP0-SP5) including a total of 19 work packages (WP). Project ‘Alloy 800H’ is defined for NRG’s contribution to tasks 4.2.1 and 4.2.2 within the work package 4.2 (WP42: High temperature alloys and instrumentation) of SP4. The goal of WP42 is to study materials suitable for application in heat transfer circuit components for (V)HTR reactor systems, i.e. (i) gas to steam generator unit (SGU) with a maximum operational temperature between 650 -700^{o}C and (ii) gas to gas intermediate heat exchanger (IHX) with a maximum operational temperature between 700 - 850^{o}C. Alloy 800H is identified as a candidate material for IHX components.

1.2 Scope of the Alloy 800H project

The objective of ‘Archer alloy 800H’ is to characterize the reference mechanical properties (tensile and creep/creep-fatigue interactions) of the alloy 800H base and weld material at temperatures ranging from RT to 800^{O}C and to carry out the basic microstructural studies. The primary focus was to study the base material properties. According to an agreement reached between the project partners, testing of weld material is conditional and depends upon availability of both leftover material and additional budget. No irradiation experiments will be performed within this project. Because of the limited budget of this project, during the first ARCHER progress meeting in Julich, it was agreed the following:

- tensile testing to be performed at 3 different temperatures in air environment.
- low cycle fatigue (LCF) tests without and with a hold time at the peak stresses (for creep-fatigue interaction study) to be performed at one single temperature in air environment and at 4 different strain ranges.
- limited scale microscopic studies using optical microscopy (OM), scanning electron microscopy (SEM) and transmission electron microscopy (TEM) to be performed.
- the results of the tensile and fatigue/creep-fatigue interaction tests, including the results from the microstructural investigation to be reported.

1.3 Activities planned

The following activities are planned within this project as a NRG contribution to tasks 4.2.1.and 4.2.2.

1. Material procurement: Alloy 800H, both base material (BM) and weld material (WM) to be procured for mechanical testing and microscopy investigation.
2. Specimen fabrication: Limited number of tensile and LCF specimens to be manufactured for mechanical testing.
3. Microscopy work: Limited microstructural studies (OM +SEM) to be used for material characterization.
4. Mechanical testing: Tensile and Low Cycle Fatigue (LCF) + hold time testing to be performed for creep-fatigue interaction phenomena studies in reference material state.
5. Reporting: The mechanical testing results and the micrographs to be analyzed and reported.

2 Experimental

2.1 Material

ThyssenKrupp VDM, one of the partners of the Archer project, supplied the alloy 800H (base and weld) material. Two plates are received by NRG for testing purposes: a 100 mm x 150 mm x 16 mm alloy 800H base material plate (Figure 2.1 (a)) and a 100 mm x 300 mm x 16 mm tungsten inert gas welded (WIG) alloy 800H material plate (Figure 2.1 (b))

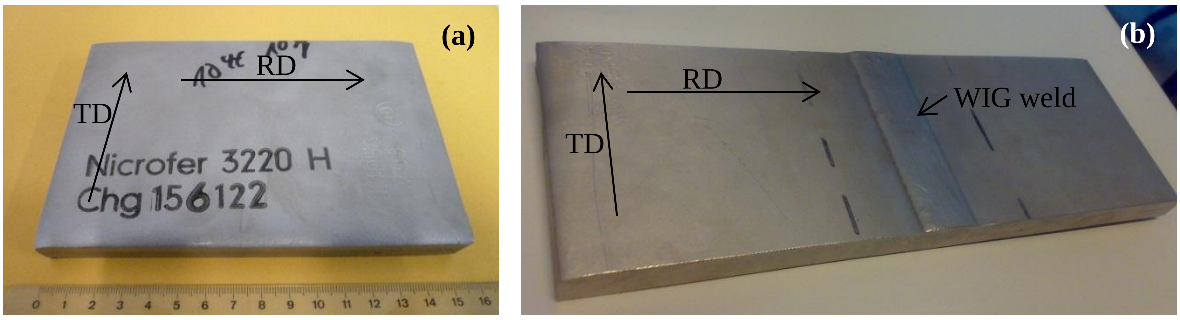

Figure 2.1 Alloy 800H (a) base material and (b) welded material received from ThyssenKrupp VDM.

The material data sheets supplied by ThyssenKrupp VDM for base and weld material are given in Appendix A. Details on the composition and the mechanical properties of these particular heats can be found in the sheets. General overview about the high temperature alloys produced by ThyssenKrupp, such as alloy characteristics, composition, heat treatments, designations and standards, physical properties and mechanical properties can be found in reference (1).

2.2 Mechanical characterization

2.2.1 Tensile tests

The tensile tests are performed on Instron servo-mechanic machine equipped with a 10 kN dynamic load cell and a high temperature furnace, with maximum operating temperature of 1100^{o}C. The temperature of the furnace can be controlled precisely within ±2^{o}C. All the tests are done in accordance with ASTM E8M. The tensile tests are performed at a constant actuator velocity, resulting in an initial strain rate of $5x10^{-4}$ s^{-1}. The specimen geometry of the NRG tensile test specimen is given in Figure 2.2.

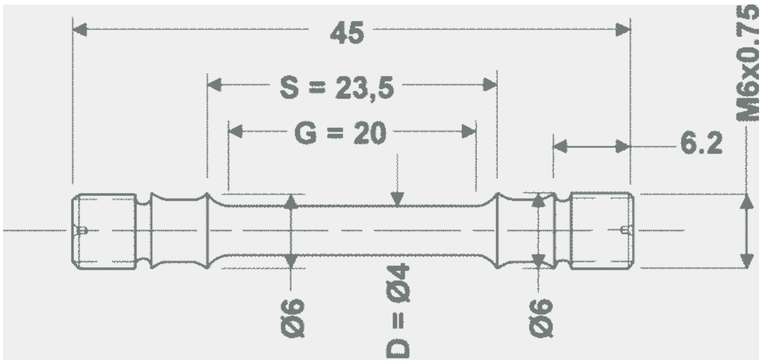

Figure 2.2. Geometry of the tensile specimen. Dimensions are in mm.

2.2.2 Low-cycle fatigue (LCF) test

The LCF tests with and without hold time are performed on the Instron servo mechanic machine equipped with a 10 kN dynamic load cell and a high temperature furnace - same as mentioned above. Strain controlled LCF test are performed using an axial, high temperature capacitive extensometer for the strain measurement. The furnace has custom cut-outs for the extensometers, which are controlled by Eurotherm 900EPC series temperature controllers. The LCF tests are performed in accordance with ASTM E606-92. The specimen geometry of the NRG LCF test specimen is given in Figure 2.3.

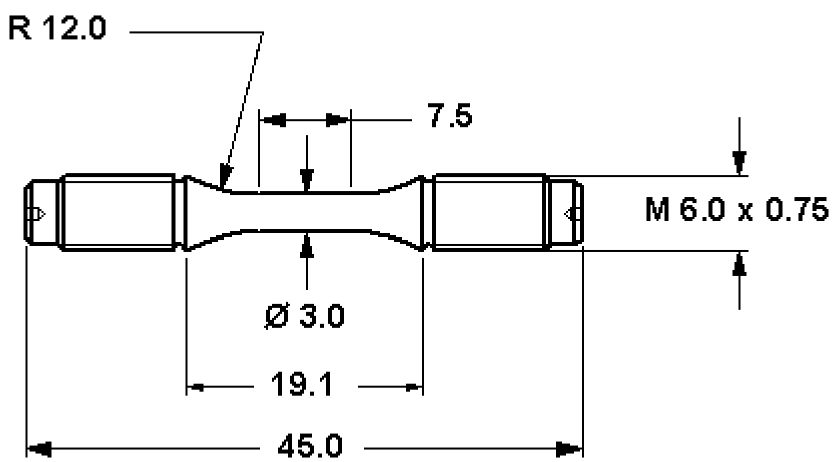

Figure 2.3. Geometry of the LCF specimen. Dimensions are in mm.

All the LCF tests are performed in air at 800°C and at a strain rate of $1x10^{-3.}$ The cyclic strain ratio R ($\varepsilon_{min}/\varepsilon_{\max}$) of -1 is employed. The applied total strain ranges ($\Delta\varepsilon_{tot}$) include 1.5%, 1.2%, 0.9% and 0.6%. Tests are performed without and with a hold time (HT) only in tension (for creep-fatigue interaction study) at the 4 strain ranges given above. The number of cycles for 50% drop (N_{50}) in the initial stress is used as a failure criterion for end of life cycles (N_f). Once the LCF test is finished (i.e.

after reaching N_{50}) the sample is separated into two pieces by monotonic loading under tensile stress. Figure 2.4 shows the broken LCF sample at the end of the test.

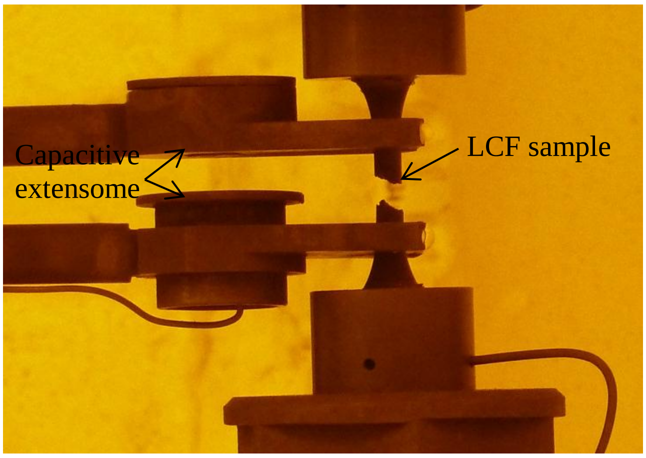

Figure 2.4. Picture of the broken sample (P417) at the end of the LCF test. In the figure, high temperature capacitive extensometer used for the axial strain measurement can also be seen.

2.2.3 Test matrix

During the 1st ARCHER progress meeting in Julich, it was agreed between the partners that NRG will perform in total 3 tensile tests and 8 LCF tests with/without hold time on base material. Although testing of weld material was not committed during this first meeting, it was agreed to eventually perform weld metal characterization in case budget would be available after base material testing campaign is completed. Table 2.1 shows the test matrix of tensile and LCF tests accomplished in this project. The specimens are cut using electro discharge machining (EDM). Initially, tensile and LCF samples were cut in the transverse direction (TD) from the base material that was delivered at first. The weld material which was received later was welded across the rolling direction (RD) of the plate. To be able to compare directly the results between the base and weld materials, it was decided to re-cut both base and weld specimens in RD from the welded plate.

Table 2.1. Test matrix of tensile and LCF tests performed in this project.

Test name		**Tensile**	**LCF in air at 800 ^{o}C**	
			No-HT	**HT (1000 sec)**
No. of samples	Base TD	3 (RT, 700 and 800 ^{o}C)	-	-
	Base RD	3 (RT, 700 and 800 ^{o}C)	4	8
	Weld RD	3 (RT, 700 and 800 ^{o}C)	-	-

2.3 Microscopic examination

Preliminary microscopic studies were performed on base alloy 800H material using OM, SEM and TEM. Weld material was investigated only by SEM. Details about the microstructure are discussed in the next section.

3 Results

3.1 Tensile tests

The stress-strain results from tensile tests performed at room temperature (RT), 700^{o}C and 800^{o}C are compared for base TD, base RD and weld RD specimens in Figure 3.1, Figure 3.2 and Figure 3.3, respectively. The 0.2% offset Yield Stress (YS), Uniform plastic Elongation (UE), Total Elongation (TE) and strength data from specific plastic strain intervals are calculated from the load-displacement curve. The fracture elongation and reduction of area are measured on the specimen halves after testing. The total elongation data obtained from the load-displacement curves show no systematic deviation from the measured fracture elongation (see Figure 3.4), though some scatter exists. The total elongation data obtained from the load-displacement curves are used in this report. The specimen data for all the tests are given in the Appendix B.1.

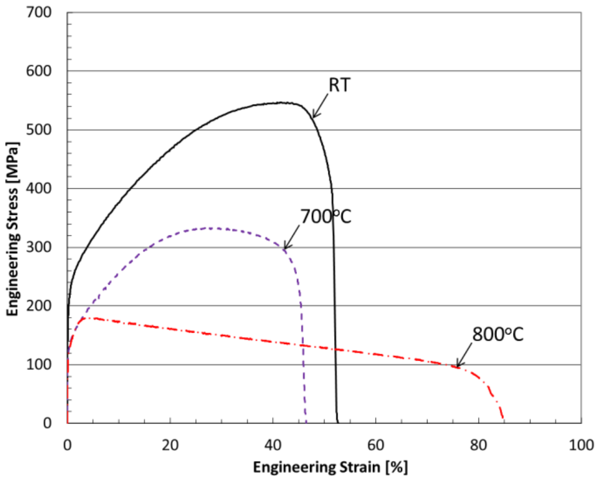

Figure 3.1. Engineering stress-strain curves of the base material specimens in transverse direction (TD) at 3 different temperatures.

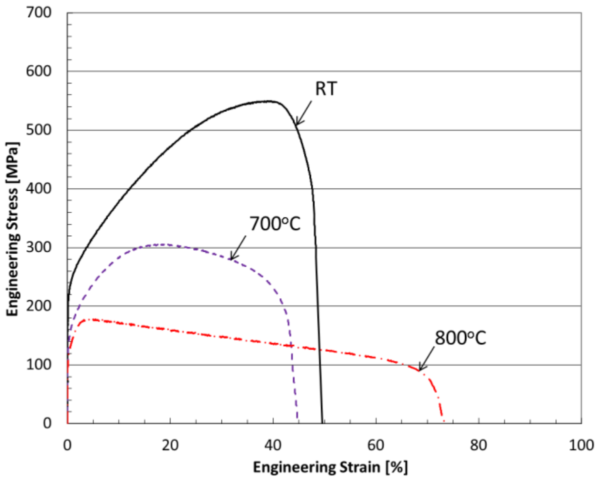

Figure 3.2 Engineering stress-strain curves of the base material specimens in rolling direction (RD) at 3 different temperatures.

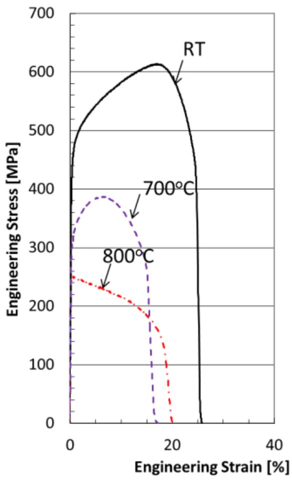

Figure 3.3. Engineering stress-strain curves of the weld material specimens in rolling direction (RD) at 3 different temperatures.

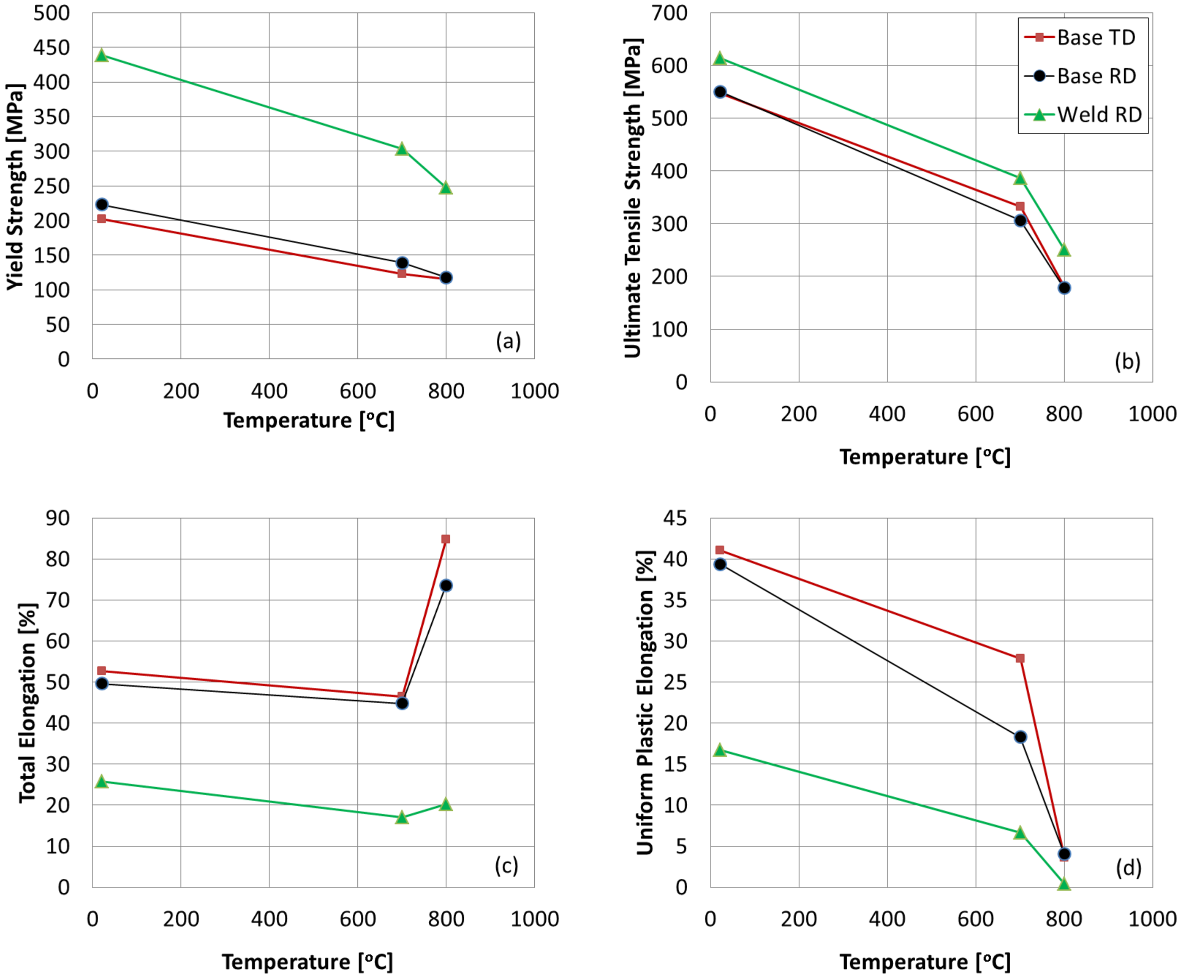

Figure 3.4. Comparison of (a) yield strength, (b) ultimate tensile strength, (c) total elongation and (d) uniform plastic elongation properties as a function of temperature for base TD, base RD and weld RD materials.

As can be noticed in Figure 3.4, the tensile properties of base materials in rolling and transverse directions are very similar at all 3 temperatures - RT, 700°C and 800°C except visible difference in UE at 800°C. However, there is considerable difference between base and weld material properties. A substantial drop in strength properties is observed at 700°C and 800°C compared to RT values in both base and weld tests. The drop in UTS and UE (as well as work hardening regime) is more pronounced between 700 to 800°C (Figure 3.4 (b)). Relatively small reduction in TE is observed in 700°C tests of base materials compared to RT tests. Results at 800°C showed significantly higher ductility for base material tests. However, only a very small uniform plastic elongation regime is observed in all the tests at 800°C.

3.2 Low cycle fatigue (LCF) tests

LCF tests are performed on the base material samples with and without hold time (HT) at 800°C at four different total strain ranges ($\Delta\varepsilon_{tot}$) i.e. 0.6%, 0.9%, 1.2% and 1.5%. The primary objective is to study the influence of the hold time on strain-life behavior of this alloy in order to understand the creep-fatigue interaction phenomenon. Consequently, the LCF results including cyclic stress-strain behavior, evolution of maximum positive and negatives stresses and the strain-life behavior are compared between tests with no-hold time and with 1000 sec hold time in tension. All LCF tests data are given in the Appendix B.2.

3.2.1 Cyclic stress-strain behavior

The cyclic stress-strain behavior of 0.6% total strain range specimens tested without hold time and with 1000 sec hold time in tension are shown in Figure 3.5 (a & b), respectively. No hold times are applied in compression. In the figures, only 4 cycles (i.e. cycle number 2, the cycle in which the saturation stress is reached, and the cycles in which the peak tensile stresses (σ_{max}) are dropped by 25% (N25) and 50% (N50)) are shown for clear visualization of the curves. A considerable strain softening can be seen in all the tests. In case of hold time tests, a clear drop in the σ_{max} to σ_{Rmax} is observed during the hold period at the maximum tensile strain (ε^{t}_{max}) indicating a clear stress-relaxation behavior of this material at 800°C. The influence of the tensile hold time on the fatigue life is shown later in section 4.2.

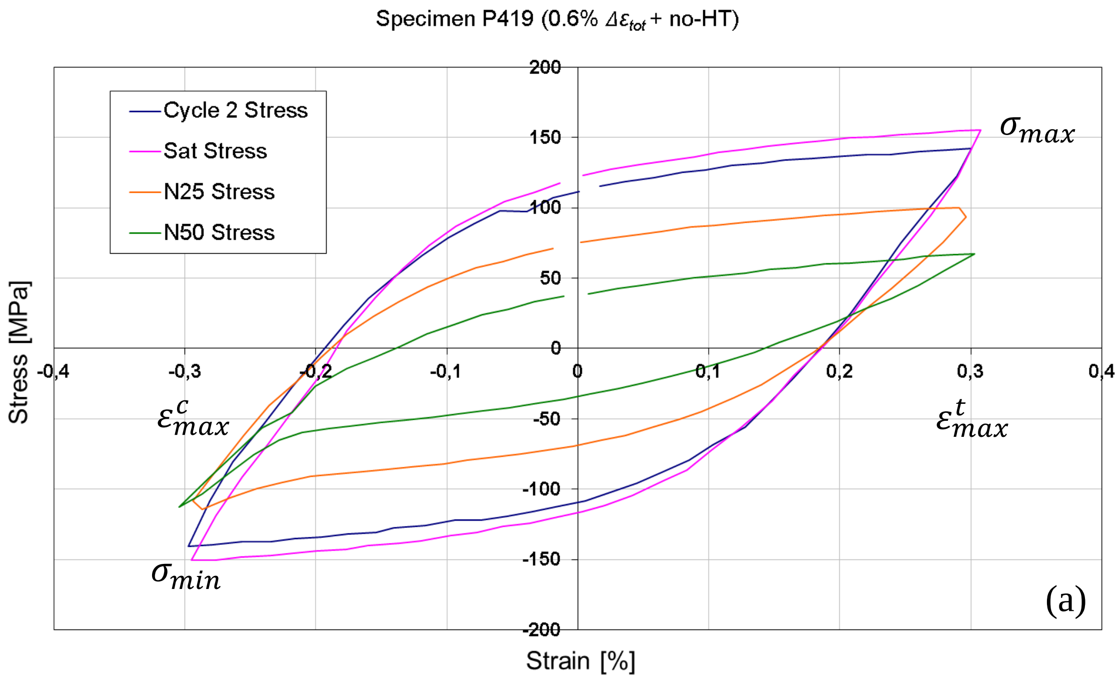

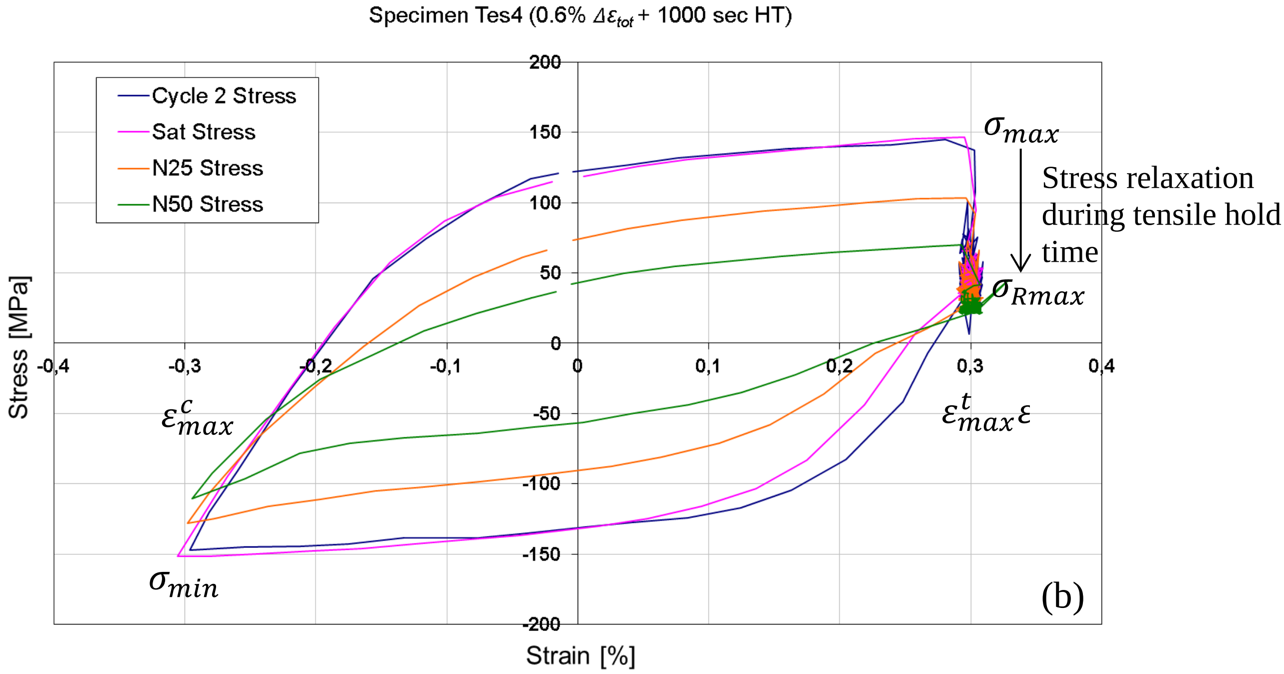

Figure 3.5. Cyclic stress-strain behavior of 0.6% total strain range specimens at 800°C (a) without hold time and (b) with 1000 sec hold time in tension.

3.2.2 Evolution of the maximum cyclic tensile and compressive stresses and influence of the hold time

Figure 3.6 (a, b, c & d) compares the evolution of the maximum cyclic tensile and compressive stresses (σ_{max} & σ_{min}) as a function of the number of cycles for each strain range. In all the tests, a slight hardening is observed during the first few cycles before the stress reaches a saturation point, called 'saturation regime'. Then a plateau in the stress is observed. Finally, a regime of cyclic softening is detected as the test progresses after the plateau regime. Various regimes of the curve are shown in Figure 3.6 (a). The maximum tensile and compressive stresses are symmetric until the start of cyclic softening behavior at all strain ranges for both no-HT and HT tests. The rate of softening in tensile peak stress is more than the compressive peak stress after the onset of cyclic softening. It is observed that the saturation stress increases with increasing the total strain range in all the tests.

In addition to the above common observations in no-HT and HT tests, a clear influence of the hold time is seen on the evolution of maximum cyclic tensile and compressive stresses and total fatigue life. First of all, the onset of softening starts much earlier than the no-HT test in both tensile and compressive regimes. Relatively shorter plateau regime is seen in all 1000 sec HT tests. Moreover, softening rate of maximum tensile stress in the cyclic softening regime is slow in all 1000 sec HT tests. Contrastingly, in general more rapid softening after a comparatively long plateau is detected in case of no-HT tests. The difference could be explained due to the extra damage contribution introduced by the stress relaxation in HT tests.

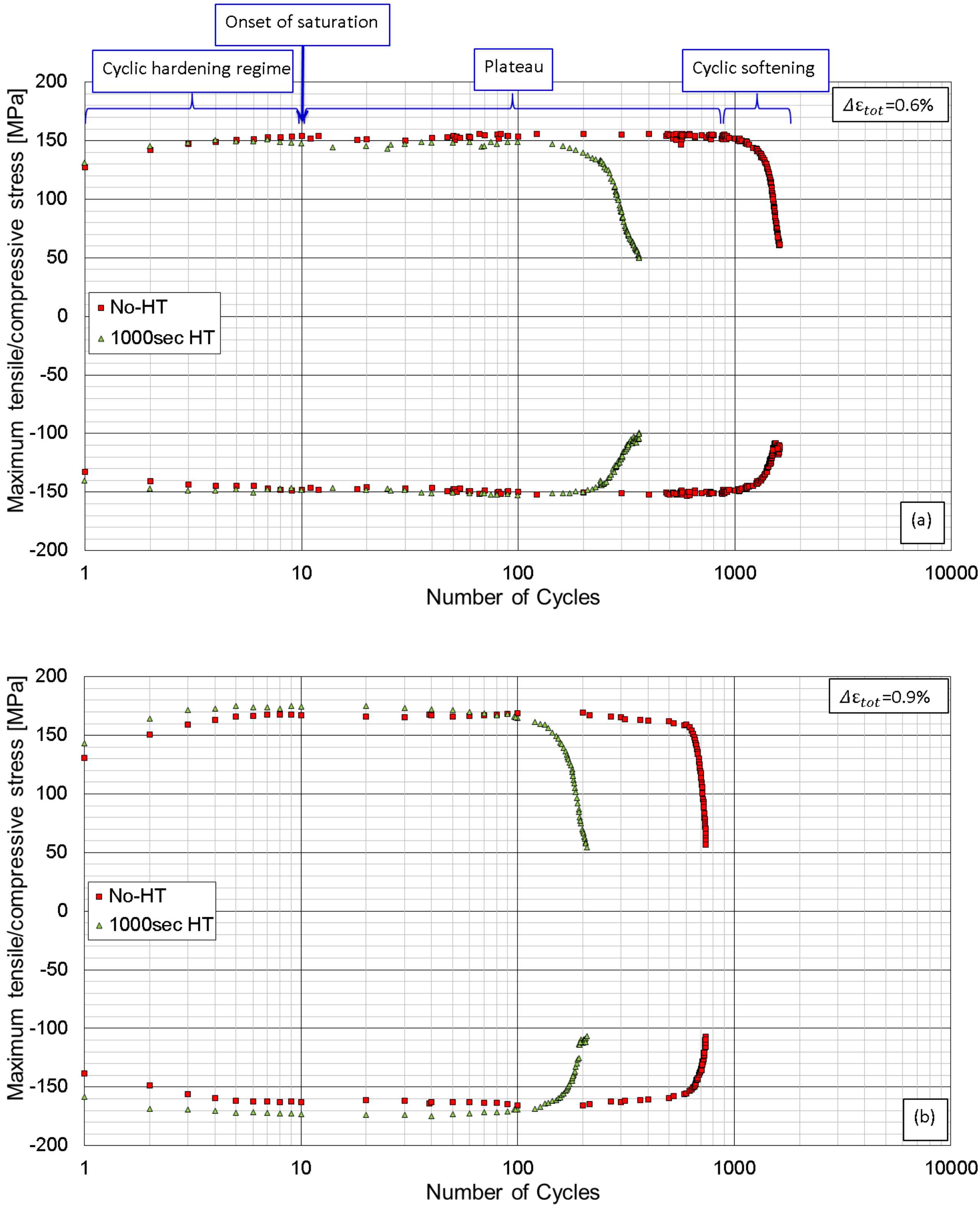

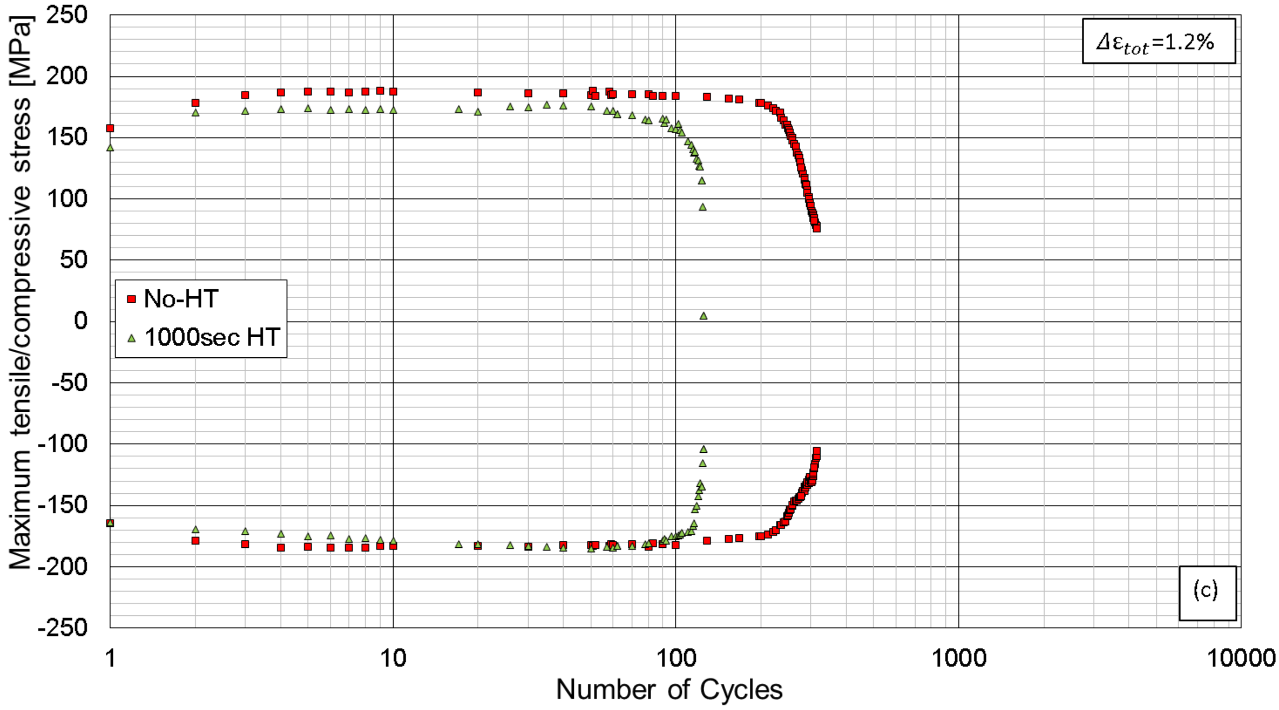

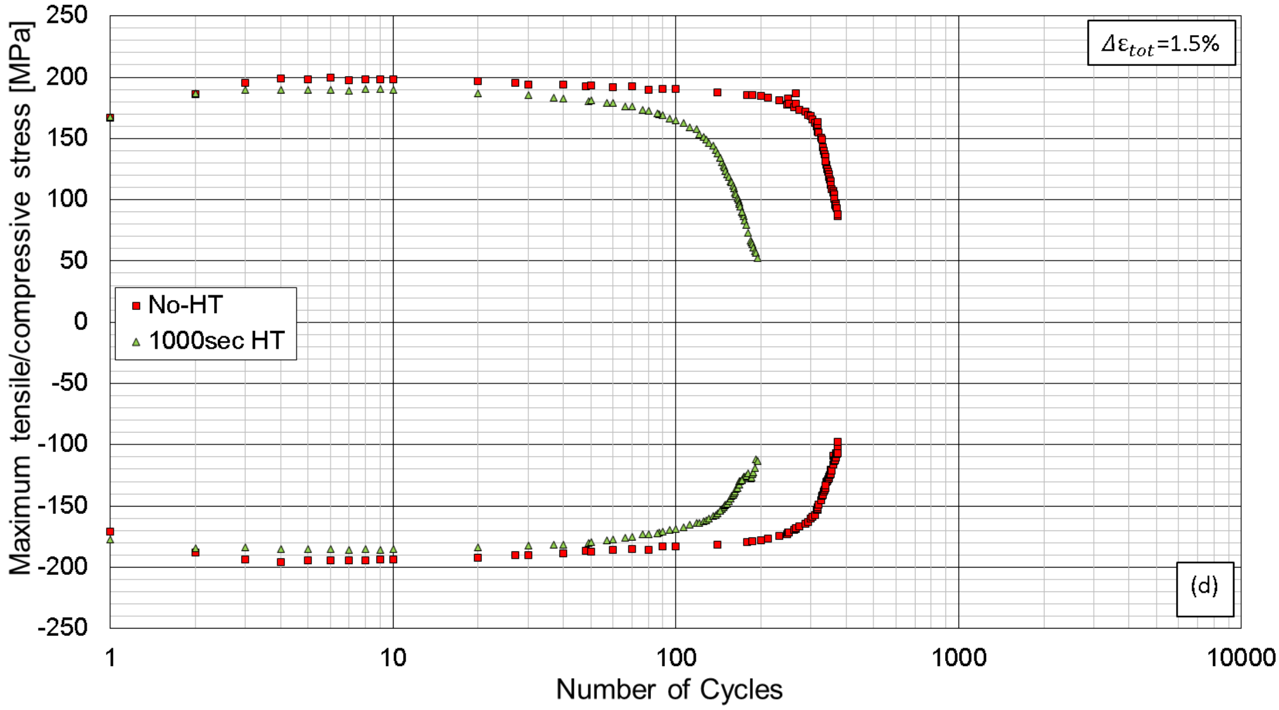

Figure 3.6. Comparison of evolution of maximum tensile and compressive cyclic stresses (σ_{max} & σ_{min}) between no-hold time tests and tests with 1000 sec hold time in tension at (a) 0.6%, (b) 0.9%, (c) 1.2% and (d) 1.5% $\Delta\varepsilon_{tot}$.

3.3 Microstructure of Alloy 800H base ans weld materials

3.3.1 Microstructure of Alloy 800H base material

Samples are cut from the Alloy 800H base material (shown in Figure 2.1(a)) and mounted in a specimen holder using epoxy resin. Consequently, the samples are first ground on a series of abrasive papers starting from grit sizes of 320, 400, 600 to P2400 and then polished using 6 micron and 1 micron diamond paste. Finally, samples are etched for 5 sec in Marble's Reagent (10 gr $CuSo_4$ +50 ml HCL+ 50 ml H_2O). Two drops of H_2SO_4 is added to increase the activity of the etchant. Immediately after etching the sample are rinsed with water and then cleaned with ethanol. Using this method allowed for very good resolution of the microstructure of this alloy. The optical micrographs of the base Alloy 800H material are shown in Figure 3.7.

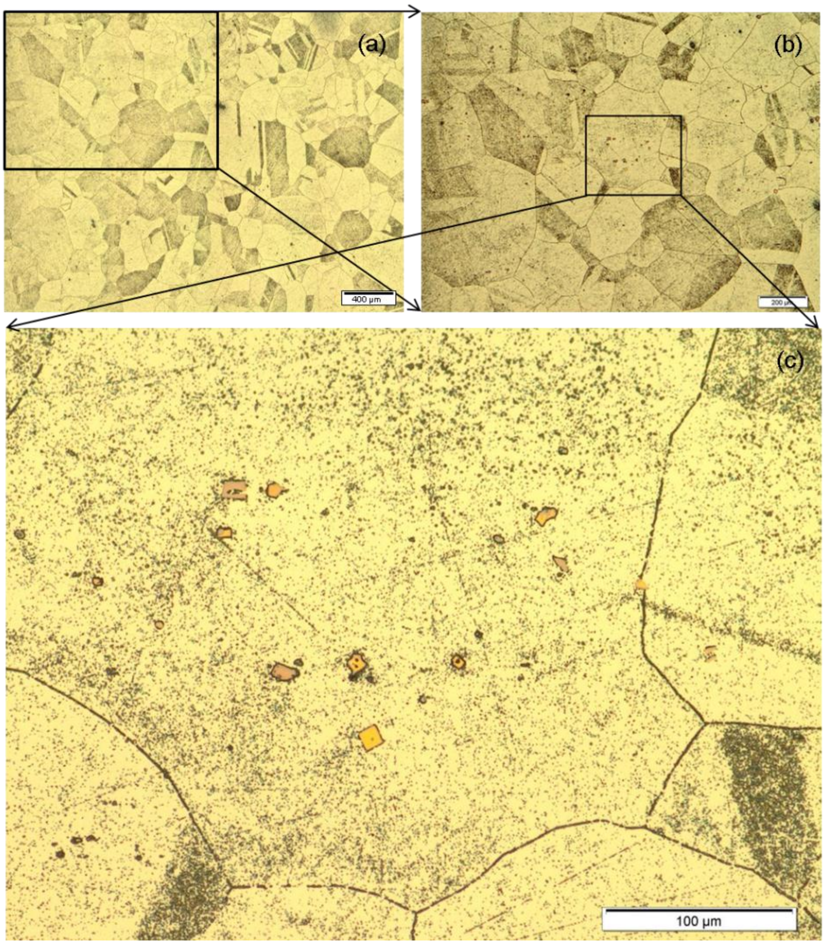

Figure 3.7. Microstructure of the Alloy 800H base material taken by optical microscope. Figures (a and b) show the overall grain structure and (c) shows a uniform distribution of the γ' precipitates. Few big cuboid shaped Ti(C,N) precipitates can also be seen in the figure (c). Samples are etched for 5 sec in Marble's Reagent (10 gr $CuSo_4$ +50 ml HCL+ 50 ml H_2O) mixed with two additional drops of H_2SO_4 for increased activity of the etchant.

The microstructure reveals a large equiaxed grains (γ phase) with uniform distribution of ordered γ' precipitates (Ni_3Al) throughout the microstructure. Few big cuboid shaped Ti(C,N) precipitates can also be seen in the Figure 3.7 (c). The mean grain size of the base material, in the investigated sample measured by linear intercept method is ASTM grain size 1.9 (167 μm).

A TEM study was performed on the base material using extractive replica method. This replica method is commonly used to extract the precipitates for further microscopic analysis. After grinding and polishing of the sample (as mentioned previously) a selective etching is performed using 5% bromine solution. A thin carbon layer is then sputtered on to the etched surface of sample in vacuum. The carbon layer (together with the precipitates) is removed out of the surface by dipping in 10% bromine solution for few minutes. This thin replica is then carefully cleaned in alcohol and eventually placed on a copper grid for TEM analysis of the precipitates.

Preliminary micro-analysis of the precipitates performed using EDS detector in the TEM indicated presence of the Ti, Cr, Fe, Cu, Ni, Al and Si peaks (Figure 3.8). No quantitative composition analysis is performed here. Presence of the Cu peaks might be coming from copper grid whereas C peak can be coming from either replica or metal carbide precipitates of type MC, $M_{23}C_6$, M_6C. For example, presence of clear Ti and C peaks seen in Figure 3.8 (a,b) indicate the possible presence of TiC precipitate. Ni, Ti and Al peaks indicate the presence of Ni_3Al or $Ni_3(Al,Ti)$ precipitates (though Ni peaks are overlapping with the Cu peak leading to a single broad peak). A future TEM analysis is needed to fully characterize the precipitates present in this alloy.

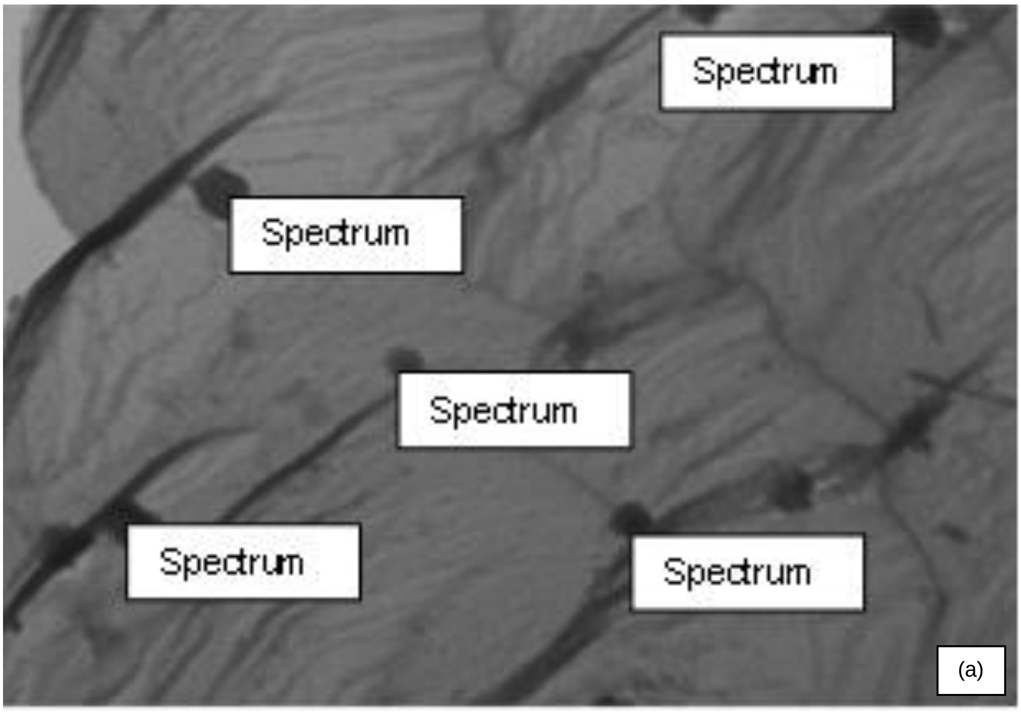

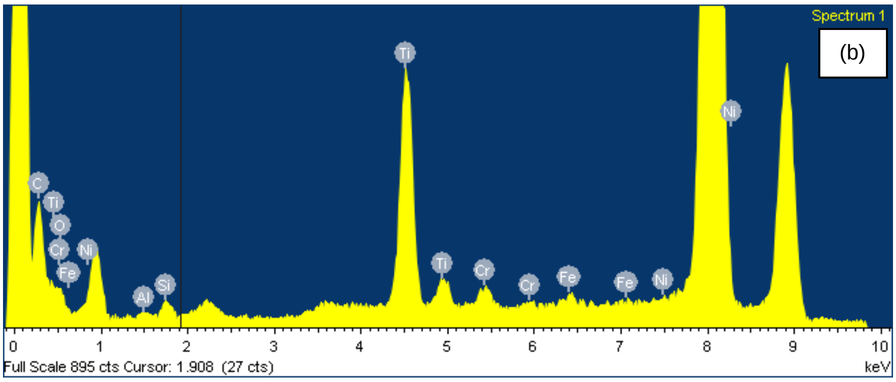
Spectrum 1
(b)
Ti
Ni
C
Ti
O
Cr
Ni
Fe
Al
Si
Ti
Cr
Cr
Fe
Fe
Ni
0 1 2 3 4 5 6 7 8 9 10
Full Scale 895 cts Cursor: 1.908 (27 cts)
keV

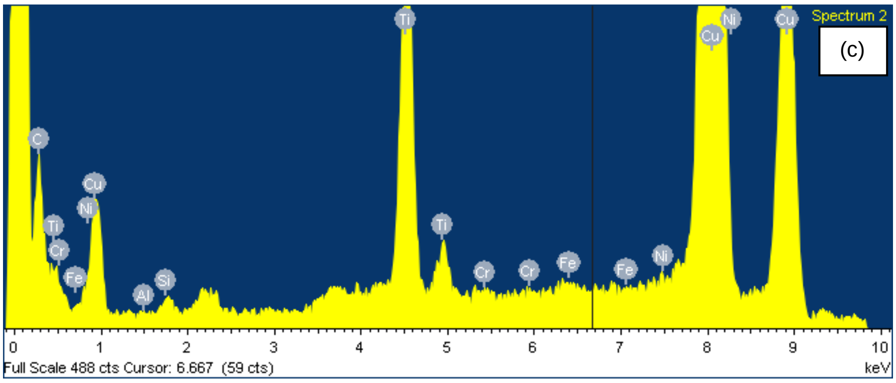
Spectrum 2
(c)
Ti
Ni
Cu
Cu
C
Cu
Ni
Ti
Cr
Fe
Al
Si
Ti
Cr
Cr
Fe
Fe
Ni
0 1 2 3 4 5 6 7 8 9 10
Full Scale 488 cts Cursor: 6.667 (59 cts)
keV

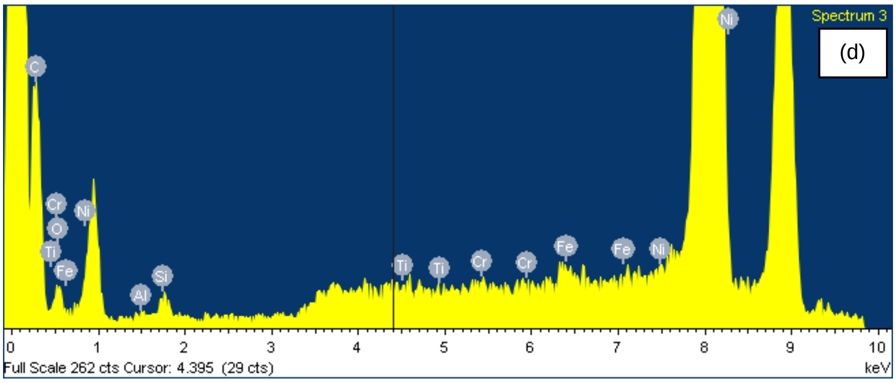
Spectrum 3
(d)
Ni
C
Cr
Ni
O
Ti
Fe
Al
Si
Ti
Ti
Cr
Cr
Fe
Fe
Ni
0 1 2 3 4 5 6 7 8 9 10
Full Scale 262 cts Cursor: 4.395 (29 cts)
keV

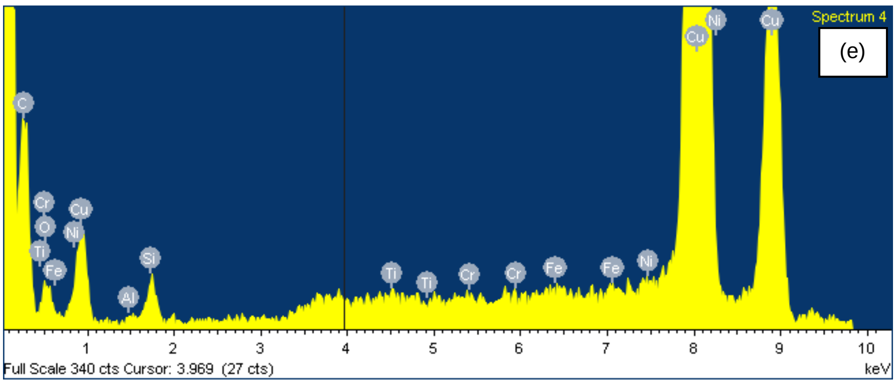
Spectrum 4
(e)
Ni
Cu
Cu
C
Cr
Cu
O
Ni
Ti
Fe
Si
Al
Ti
Ti
Cr
Cr
Fe
Fe
Ni
1 2 3 4 5 6 7 8 9 10
Full Scale 340 cts Cursor: 3.969 (27 cts)
keV

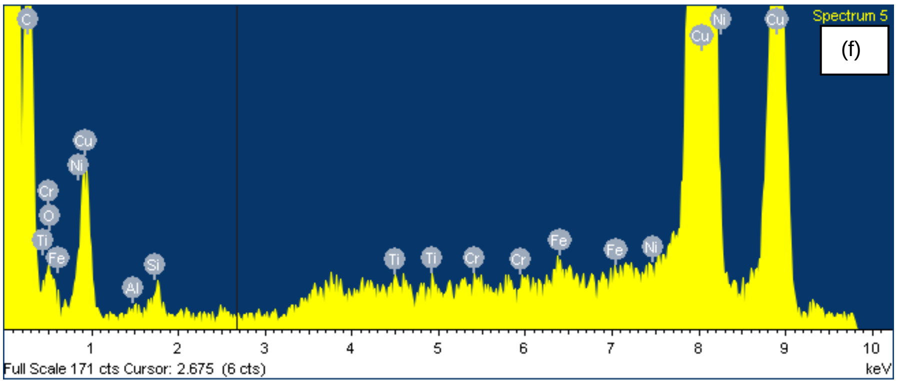

Figure 3.8. (a) TEM image of the replica taken from the Alloy 800H showing various precipitates. (b-f) EDS spectra of the precipitates shown in (a).

An EDS analysis is also performed on SEM to analyse the precipitates (see Appendix C.1). It is observed that the base material inclusions consist mainly of Si-oxides and Ti(CN) inclusions. The typical Si-oxide inclusions are smaller than 1 µm, which explains why also considerable amounts of the base material composition is measured. Most inclusions are Ti(CN), which are typically more angular-shaped and a few microns in size. This is normal for this type of material, as Ti is included as an alloying element. Apart from Ti(CN) inclusions also a few TiNb(CN) inclusions were observed. These inclusions are more spherical in shape. Again no evidence of γ' has been observed, however, using EDS only inclusions of 1 µm and larger can be identified unambiguously.

3.3.2 Microstructure of Alloy 800H weld material

Preliminary microscopic studies are performed on the weld Alloy 800H material using OM and SEM techniques. The samples are prepared perpendicular to the welding direction as shown in Figure 3.9. Preparation of the sample is done by standard metallographic methods and colloidal silica final polish. Etching is performed at room temperature for 3 minutes in a V2A etch for a general etch of the microstructure (100ml Demi-Water, 100cl conc. HCl, 10ml conc HNO_3, 0.3ml Vogels-Sparbeize). The optical micrograph of the weld cross section revealing the top 5 weld passes are shown in Figure 3.10 (a). The grain structure was clearly resolved in the base material part similar to the previous observations in Section 3.3.1. However, the grains were not resolved in the weldment. Base-weld fusion line (FL) showing dendritic structure along the fusion line is visible in Figure 3.10 (b). The dark spots in the BM are results of etching around TiC or Ti(CN) inclusions.

Grundwerkstoff:	Nicrofer 3220 H	Schweißzusatzwerkstoff:	S 7020 So 3	Ø 1,2 mm
Charge:	156122	Charge:	126161	
Werkstoffnummer:	1.4948	Werkstoffnummer:	2.48066	
Gas:	AW 2	FA:	103442167	
Länge:	500 mm	Prüfdatum:	13.05.2011	

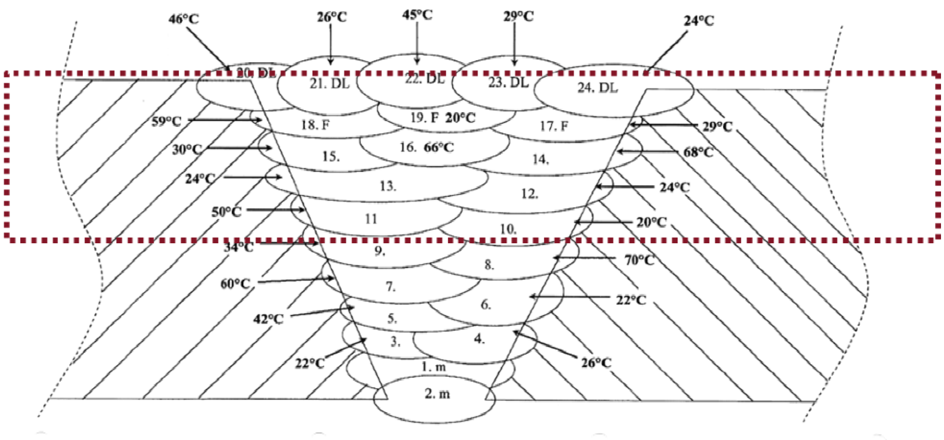

Figure 3.9. A schematic of weld execution according reported weld procedure 3266. Cut sample is indicated by dotted red line.

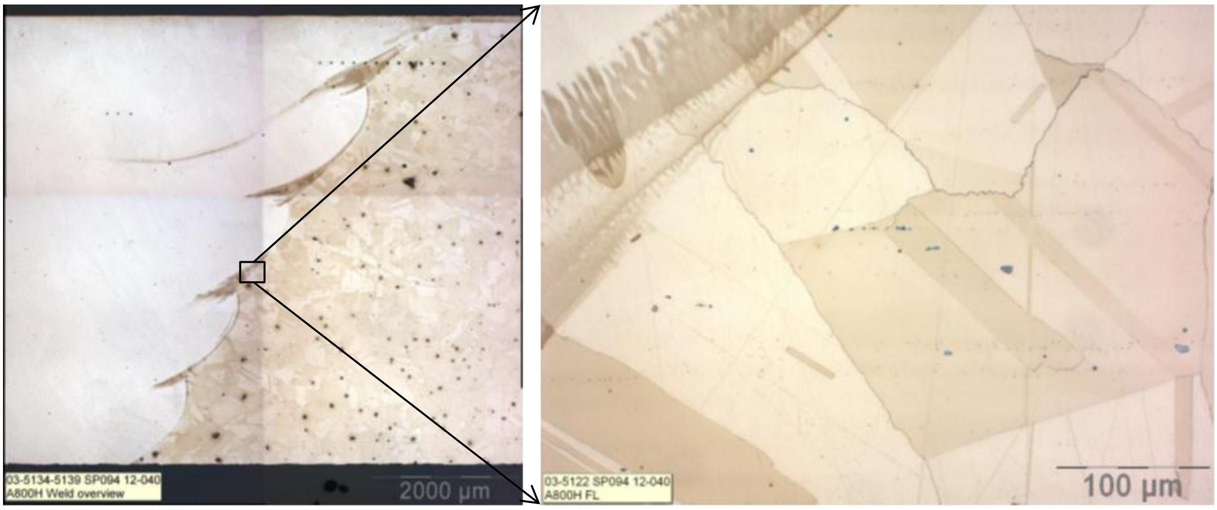

Figure 3.10. (a) Optical micrograph of the weld cross section showing the top 5 weld passes (weld beads 10-23 in Figure 3.9) out of the 11 reported in the welding procedure. (b) Zoom in on the base-weld fusion line (FL) showing dendritic structure along the fusion line. The dark spots in the BM are results of etching around TiC or Ti(CN) inclusions.

EDS analysis is performed in SEM on both base and weld materials. The results of the overall EDS analyses of the weld and base material are reported in Table 3.1. The certificate values are added as well for convenience.

Table 3.1. Results of EDS analyses of base and weld materials in comparison with material certificate values (given in italic).

	Chemical composition														
	C	S	P	Cr	Fe	Ni	Mn	Si	Ti	Nb	Cu	Mg	Co	Ta	Al
Nicrofer 3220H base material															
1.4958 base mat	*0.06*	*<0.002*	*0.010*	*20.5*	*46.7*	*30.5*	*0.7*	*0.50*	*0.34*	*0.01*	*0.1*	*Nd*	*0.1*	*nd*	*0.27*
1.4958 base mat-**EDS**	Below EDS analyses limits			**21.2**	**46.7**	**30.3**	**0.7**	**0.5**	**0.3**	**0.0**	**0.0**	**Nd**	**0.0**	**Nd**	**0.2**
Filler material															
2.4806 filler	*0.003*	*0.002*	*0.002*	*20.4*	*0.2*	*72.9*	*3.2*	*0.11*	*0.32*	*2.7*	*0.01*	*0.002*	*<0.01*	*0.01*	
2.4806 weld mat-**EDS**	Below EDS analyses limits			**20.8**	**3.6**	**69.5**	**3.1**	**0.1**	**0.3**	**2.7**	**0.0**	**0.0**	**0.0**	**0.0**	**0.0**

Several inclusions are analysed in the weld metal as well. All data are included in Appendix C.2. A summary of the results is given below.

A high concentration of small spherical inclusions is observed in the weld metal. The size is in the order of 1µm and smaller. Most of these inclusions are NbTi-inclusions. A high concentration of Mg is measured in some of the inclusions. No other oxide inclusions are observed in the weld metal, which can be expected considering the applied welding process . GTAW is known to result in clean weldments.

The observed Nb-Ti inclusions can be expected because of the presence of Nb in the weld filler metal and Ti in both the filler and the base material. Normally, it is expected that Ti forms oxides during the welding process. However, in this case this appears to be only a limited process as Ti is still observed in the inclusions. This indicates a good shielding of the weld pool form oxygen from the environment. No γ' are observed as in the case of base material.

3.3.3 Hardness Alloy 800H base and weld material

Figure 3.11 shows the HV1 Hardness profiles measured 1 mm below the cap and 1 mm below the halfway the weld. The hardness profile starts halfway the weld and stops in the base material. The average hardness in Weld, HAZ and BM are given in the table as well.

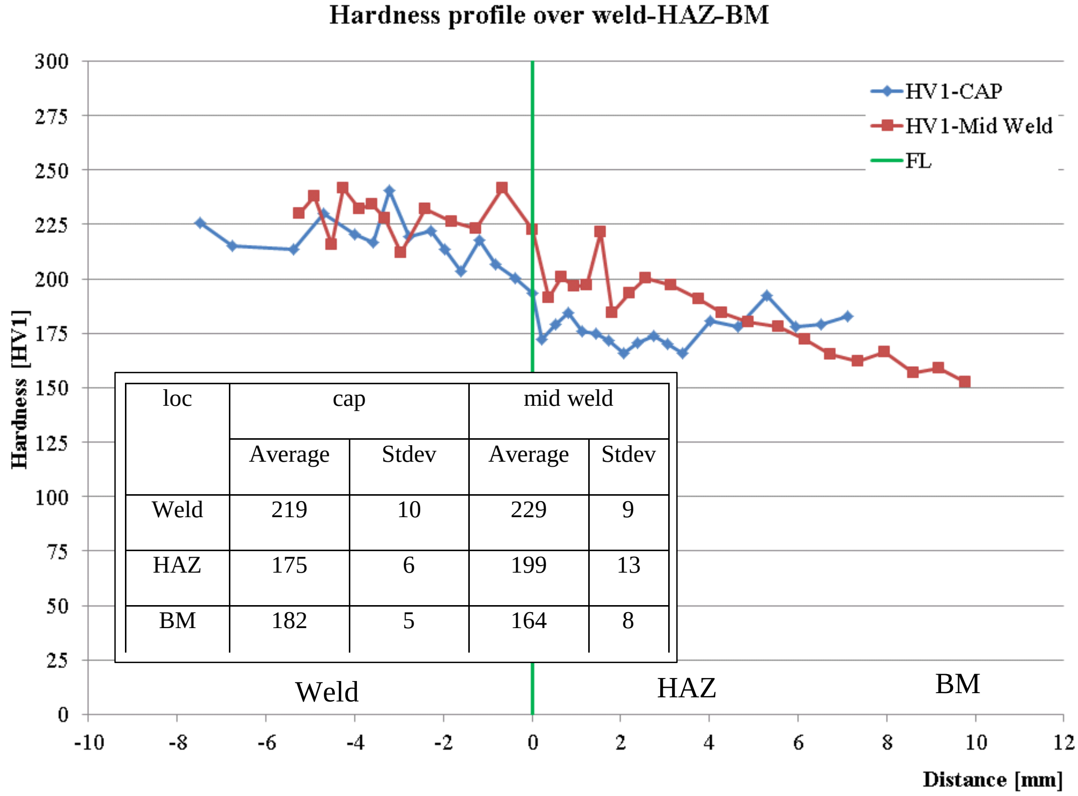

loc	cap		mid weld	
	Average	Stdev	Average	Stdev
Weld	219	10	229	9
HAZ	175	6	199	13
BM	182	5	164	8

Figure 3.11. HV1 hardness profiles over weld-HAZ-BM.

The hardness profiles in Figure 3.11 show that the weld metal hardness is similar for the weld cap and the centre of the plate (mid weld), namely 219-229 HV1. In the HAZ however, the hardness in the centre of the plate tends to be a little higher than at the weld cap, namely 175 ± 6 HV1 versus 199 ± 13 HV1. On the other hand, the base material at the cap side tends to have a little higher hardness than the plate centre, namely 182 ± 5 HV1 versus 164 ± 8 HV1. This might be explained with the rolling process of the plate - possibly residual stresses can be present in the plate.

4 Discussion

4.1 Tensile properties

Alloy 800H microstructure contains hard cuboid γ' prime precipitates (ordered LI_2 structure) distributed in relatively soft γ-matrix (disordered FCC structure). The higher strength in γ' is a result of super dislocations in LI_2 structure whose burgers vector (2b) is double the burgers vector (b) of normal dislocation in a FCC structure. These super dislocations are 4 times more energy expensive because the energy required to move a dislocation is proportional to the Gb^2 value. There are two contributing phenomena to the strength properties i.e. solution hardening in the γ-phase and precipitation hardening resulting from the hindrance of dislocation motion by γ' precipitates. The relative contributions of these two (solid solution and precipitation) hardening mechanisms in this alloy determines strength and ductility properties. For example, the contribution from solution hardening in γ phase diminishes with increase in temperatures because of the thermally activated flow softening behavior resulting from the increased dislocation velocity at higher temperatures. This explains the decrease in YS and UTS with increase in temperature (shown in Figure 3.4 (a & b)).

On the other hand, it is know from the literature reports (2) that this drop in YS for Alloy 800H becomes negligible between 500-800°C due to the increase in strength of the γ' phase with temperature increase.. This behavior is known as a flow stress anomaly. This is because the super dislocation in an ordered LI_2 structure (γ' phase) dissociates into two super partials (normal dislocations) and an anti-phase boundary. Each of the super partial again dissociates into two partial dislocations and a stacking fault. This dissociated dislocation is initially glissile when it is in planar configuration. However, due to energetic reasons, this becomes sessile dislocation with non-planar configuration (called Kear-Wilsdorf lock) when there is sufficient thermal activation energy (i.e. at high temperatures). The drop in UTS from 700 to 800°C is steeper compared to drop from RT to 700 °C. This is because of the superior effect of flow softening with increases in temperature beyond 700°C compared to relatively small contribution of hardening coming from γ' precipitates. A very small UE with negligible hardening regime at 800°C is also because of this reason. The long elongation regime after an early onset of necking at 800°C could be a manifestation of inhomogeneous dynamic strain ageing causing the neck to extend along the gauge length. In any case the presence of uniformly distributed strong γ' precipitates at high temperatures provides the superior high temperature strength of this alloy. Comparatively, lower ductility and higher strength properties of the weld materials might be because of the sensitization of the microstructure during welding. Further microscopic investigation is needed for confirmation of this reasoning.

4.2 Creep-fatigue properties

4.2.1 Effect of the hold time on the fatigie life

From the LCF results presented in section 3.2, it is clear that introduction of a HT causes a considerable reduction in the number of cycles to failure at any given $\Delta\varepsilon_{tot}$. This effect is clearly illustrated in the strain-life diagram shown in Figure 4.1. In both the no-HT and HT tests, fatigue life decreases considerably with increasing $\Delta\varepsilon_{tot}$ except for $\Delta\varepsilon_{tot} = 1.5\%$, where a slight increase in fatigue life is seen compared to $\Delta\varepsilon_{tot} = 1.2\%$. The difference in number of cycles to failure between no-HT and HT tests increases with decreasing $\Delta\varepsilon_{tot}$. From these results it is clear that creep (or stress-relaxation) plays an important role in HT tests at 800°C and its relative contribution to total damage increases with decreasing $\Delta\varepsilon_{tot}$

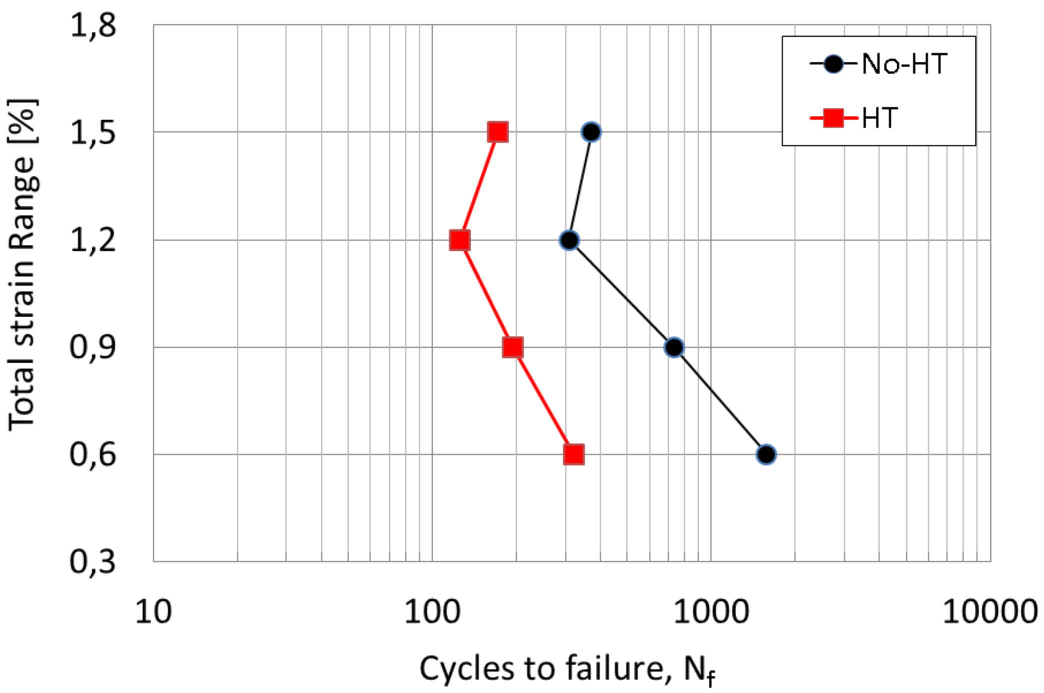

Figure 4.1. Comparison of the strain-life curves of the no-HT and HT tests at 800°C.

5 Conclusions

Results of the reference mechanical and microscopic characterization of Alloy 800H base and weld materials are presented in this report. Tensile tests on Alloy 800H base and weld materials were performed at RT, 700°C and 800°C. In both base and weld materials, a considerable decrease of the strength properties (YS and UTS) is observed with increasing the temperature. Particularly, the reduction in UTS from 700°C to 800°C is pronounced. An another observation is that the ductility (% total elongation) increases considerably from 700°C to 800°C while the uniform plastic elongation is considerably reduced. These observations are attributed to the changes in the relative contributions of the two (solid solution and precipitation) hardening mechanisms in this alloy.

The LCF tests are performed on base material with no-HT and 1000 sec HT in tension at 800°C at 4 different total strain ranges. No LCF tests on weld material are performed. Introduction of HT reduces the fatigue life substantially at all strain ranges (with maximum reduction at the lowest strain range) indicating the contribution of stress relaxation (or creep) mechanisms to the total damage at this temperature.

Preliminary microscopic studies were performed on both base and weld materials. The microstructure of the base material revealed an equiaxed grain structure of γ matrix with uniformly distributed γ' precipitates. The results from the EDS analysis of the precipitates in both base and weld materials revealed the presence of various precipitates contributing to the strengthening mechanisms in this alloy.

6 Recommendations for the future work

- It should be noted that only one test is performed at each test condition. More tests are required for the statistical representation of the data.
- Post-test microscopic investigation of the broken LCF specimens is needed for better understanding the failure mechanisms.

References

1. *High temperature alloys: Nicrofer® 3220 H/3220 HP-alloys 800 H/800 HP.* s.l. : ThyssenKrupp VDM, 2002. Material Data Sheet No. 4029.

2. *Characterization of elevated temperature properties of heat exchanger and steam generator alloys.* **J.K. Wright, L.J. Carroll, C. Cabet, T.M. Lillo, J.K. Benz, J.A. Simpson, W.R. Lloyd, J.A. Chapman, R.N. Wright.** 2012, Nuclear Engineering and Design, Vol. 251, pp. 252-260.

List of tables

Table 2.1. Test matrix of tensile and LCF tests performed in this project. 11

Table 3.1. Results of EDS analyses of base and weld materials in comparison with material certificate values (given in italic). 25

List of figures

Figure 2.1 Alloy 800H (a) base material and (b) welded material received from ThyssenKrupp VDM. 9

Figure 2.2. Geometry of the tensile specimen. Dimensions are in mm. 10

Figure 2.3. Geometry of the LCF specimen. Dimensions are in mm. 10

Figure 2.4. Picture of the broken sample (P417) at the end of the LCF test. In the figure, high temperature capacitive extensometer used for the axial strain measurement can also be seen. 11

Figure 3.1. Engineering stress-strain curves of the base material specimens in transverse direction (TD) at 3 different temperatures. 13

Figure 3.2 Engineering stress-strain curves of the base material specimens in rolling direction (RD) at 3 different temperatures. 14

Figure 3.3. Engineering stress-strain curves of the weld material specimens in rolling direction (RD) at 3 different temperatures. 14

Figure 3.4. Comparison of (a) yield strength, (b) ultimate tensile strength, (c) total elongation and (d) uniform plastic elongation properties as a function of temperature for base TD, base RD and weld RD materials. 15

Figure 3.5. Cyclic stress-strain behavior of 0.6% total strain range specimens at 800°C (a) without hold time and (b) with 1000 sec hold time in tension. 17

Figure 3.6. Comparison of evolution of maximum tensile and compressive cyclic stresses (σmax & σmin) between no-hold time tests and tests with 1000 sec hold time in tension at (a) 0.6%, (b) 0.9%, (c) 1.2% and (d) 1.5% $\Delta\varepsilon tot$. 19

Figure 3.7. Microstructure of the Alloy 800H base material taken by optical microscope. Figures (a and b) show the overall grain structure and (c) shows a uniform distribution of the γ' precipitates. Few big cuboid shaped Ti(C,N) precipitates can also be seen in the figure (c). Samples are etched for 5 sec in Marble's Reagent (10 gr $CuSo_4$ +50 ml HCL+ 50 ml H_2O) mixed with two additional drops of H_2SO_4 for increased activity of the etchant. 20

Figure 3.8. (a) TEM image of the replica taken from the Alloy 800H showing various precipitates. (b-f) EDS spectra of the precipitates shown in (a). 23

Figure 3.9. A schematic of weld execution according reported weld procedure 3266. Cut sample is indicated by dotted red line. 24

Figure 3.10. (a) Optical micrograph of the weld cross section showing the top 5 weld passes (weld beads 10-23 in Figure 3.9) out of the 11 reported in the welding procedure. (b) Zoom in on the base-weld fusion line (FL) showing dendritic structure along the fusion line. The dark spots in the BM are results of etching around TiC or Ti(CN) inclusions. 24

Figure 3.11. HV1 hardness profiles over weld-HAZ-BM. 26

Figure 4.1. Comparison of the strain-life curves of the no-HT and HT tests at 800^{o}C. 28

Appendix A

A.1 Material data sheet: Alloy 800H base material

ThyssenKrupp VDM

ThyssenKrupp

ThyssenKrupp VDM GmbH
Postfach 1251 - Kleffstr. - 58742 Altena

MPA Stuttgart Otto Graf Institut

Lieferschein

z.H. Herrn Dr. Andreas Klenk
Pfaffenwaldring 32b

DE 70511 Stuttgart

Datum 08.08.2011

Ihre Bestellung Nr. vom 04.08.2011	Unser Zeichen / Bearbeiter Kemper	Telefon-Durchwahl 02392/55-2882
Unsere Auftrags-Nr. 63818	Kontroll-Nr.	Versandstelle Werk Altena
Versand erfolgt durch Klöwer		Versandtag 08.08.2011

Pos.	Liefergegenstand	Nettogewicht	Anzahl
	Musterbleche für Versuche wie mit Frau Dr. Klöwer besprochen.		
1	Nicrofer 3220 H 149580 Chg: 156122	19,9	2
	Abm: 16 x 150 x 500 mm		
	Anlage: Werkstoffdatenblatt Werkzeugnis IM PAKET	Netto 19,9 kg	
		Brutto 20,3 kg	Pakete 1

Wir erklären hiermit,
- dass die Sendung keine verbotenen Gegenstände gemäß der Anlage zur Verordnung(EG) Nr. 2320/2002 enthält, mit Ausnahme der Güter, die gemäß den gültigen ICAO/IATA-Gefahrgutvorschriften für die Beförderung zulässig sind,
- dass Verpackung und Inhalt der Sendung aus Sicherheitsgründen untersucht werden können (z.B. Stichprobenkontrollen)

ThyssenKrupp VDM GmbH

Unterschrift des Spediteurs

ThyssenKrupp VDM GmbH
Plettenberger Strasse 2, D-58791 Werdohl
Postfach 1820, 58778 Werdohl
Telefon: (02392) 55-0, Telefax: (02392) 55-2137
E-mail:
Internet:www.thyssenkruppvdm.de

Vorsitzender des Aufsichtsrats: Dr. Michael Rademacher
Geschäftsführung: Dr. Jürgen Olbrich, Vorsitzender;
Dipl.-Wirtsch.-Ing. Gerald Priegnitz,
Dr.-Ing. Franz-Josef Wahlers
Handelsregister: Amtsgericht Iserlohn, HRB 5327
Sitz der Gesellschaft: Werdohl

Ein Unternehmen von ThyssenKrupp Steel **ThyssenKrupp VDM**

ThyssenKrupp VDM GmbH
Produktbereich Blech
…effstraße 23, D-58762 Altena
Postfach 1251, D-58742 Altena
Tel. +49 2392 552082
Fax +49 2392 552047
EMail KSawinski@TKS-VDM.THYSSENKRUPP.COM

Zertifikat EN 10204 **Nr. 31191/0** 3.2 C

Seite 1 von 1
gedruckt: 29.12.2004

ThyssenKrupp

Auftragsnr. 2329

Lieferschein

Handelsmarke **NICROFER 3220 H** **1.4958**

Herstellerzeichen

ThyssenKrupp VDM
Kleffstr. 23
- 58762 Altena

Produkt
Musterblech, warmgewalzt, lösungsgeglüht, beidseitig geschliffen, geschnitten

Spezifikation	Werkstoff
ASTM B 409-01	UNS N08810
DIN 17460 09/92	X5NiCrAlTi 31 20
SEW 470-76	X 5 NiCrAlTi 32-20
VDTÜVBL. 434/03.99	X5NiCrAlTi 31 20

Pos.	Stück	Gew [kg]	Dimension [mm]	Charge	Los	
8	63		16,000x 150,0x 500,0	156122	103258397	Probe-Nr. 793

Analyse (Gew %)

Charge	Erschmelzung	C	S	Cr	Ni	Mn	Si	Ti	Nb	Cu	Fe	P	Al	Co
156122	EO/VD	0,06	<0,002	20,5	30,5	0,7	0,50	0,34	0,01	0,10	R46,7	0,010	0,27	0,1

Stückanalyse (Gew-%)

Charge	Los	Probe-Nr.	C	S	Cr	Ni	Mn	Si	Ti	Cu	P	Al	Co
156122	103258397	793-F	0,07	<0,002	20,5	30,5	0,7	0,51	0,35	0,10	0,010	0,28	0,1

Probenzustand lösungsgeglüht		Zugversuch 1 EN 10002-1 / Querprobe										Korngrösse 1 EN 103		Rekrist.
Los	Probe-Nr.		Temp [°C]	Rp0.2 [MPa]	Rp1.0 [MPa]	Rm [MPa]	Dehnung A	[%]	A	[%]	Z [%]			[%]
103258397	793-F	1	RT	227	259	534	5	53	50	64				
103258397	793-1											1	Nr 2.5	100

Spektralanalytische Verwechslungsprüfung wurde durchgeführt: ohne Beanstandung
Dimensions- und visuelle Kontrolle durchgeführt: ohne Beanstandung
Kontrolliert: 63 Bleche 16 x 150 x 500 mm
Markierung: 1.4958 - 793

TÜ 4

Der Sachverständige des RWTÜV e.V.

LRQA Approval
Number 912097

Wir bestätigen hiermit, dass das oben aufgeführte Material in Übereinstimmung mit den Lieferspezifikationen des Auftrags ist. Klaus Sawinski, Werkssachverständiger	Zeichen des Sachverständigen Q

3 1 1 9 1 - 0 - 0

Dieses beglaubigte Prüfzeugnis darf nicht außer in Gänze ohne schriftliche Erlaubnis der herausgebenden Organisation reproduziert werden. Die Eintragung von falschen, fiktiven oder betrügerischen Angaben auf dem Zertifikat kann als Straftat nach Bundesgesetz bestraft werden.

A.2 Material data sheet: Alloy 800H weld material

ThyssenKrupp VDM
Schweißlabor

Schweißprotokoll

Prüfstück Nr.	3266

Zusatzwerkstoff

Hersteller-Bez.	**Nicrofer S 7020**	**ASTM/AWS**	
Werkstoff Nr.	2.4806	**Abmessung [mmØ]**	2,5/1,2
DIN Bezeichnung	SG-NiCr20Nb	**Chargen-Nr.**	380367

Grundwerkstoff

Hersteller-Bez.	**1. Nicrofer 3220 H**	**2. Nicrofer 3220 H**	**Blechdicke [mm]**	16
Werkstoff Nr.	1.4958	1.4958	**Nahtvorbereitung**	Hobeln
DIN Bezeichnung	X 5 NiCrAlTi 31 20	X 5 NiCrAlTi 31 20	**Nahtlänge [mm]**	500
Chargen-Nr.	156122	156122		

Schweißparameter

		Wurzellage	**Kapplage**	**Fuellage 1 - 17**	**Decklage 1 - 5**		
Stromquelle		Messer Griesh. EUROMATIG-25	Messer Griesh. EUROMATIG-25	Heissdr. Fronius Trans TIG 450	Heissdr. Fronius Trans TIG 450		
Schweißverfahren		m-WIG [141]	m-WIG [141]	v-WIG-Hd [141]	v-WIG-Hd [141]		
Stromart / Polung		DC/-	DC/-	DC/-	DC/-	/	/
Spannung	[V]	12	12	13	13		
Stromstärke	[A]	120	135	190	190		
Pulsspannung	[V]						
Grundstrom	[A]						
Pulsstrom	[A]						
Grundzeit / Pulszeit	[ms]	/	/	/	/	/	/
Frequenz	[Hz]						
Schweißgeschwindigkeit	[cm/min]	12	16	22	22		
Streckenenergie	[kJ/cm]	7,2	6,1	6,7	6,7		
Drahtgeschwindigkeit	[m/min]			1,65	1,65		
Anzahl der Raupen		1	1	17	5		
Pendelbreite	[mm]						
Zwischenlagentemperatur	[°C]	22	45	45	35		
Elektrodentyp / Ø	[mm]	WT20/2,4	WT20/2,4	WT20/3,2	WT20/3,2	/	/
Düsen Ø / -Abstand	[mm]	16/10	16/10	20/12	20/12	/	/

Hilfsstoffe

Gase	**Menge [l/min]**	**Handelsname**	**Zusammensetzung**					
WIG-Brenner	14	Argon W2	Ar 98	He	H_2 2	N_2	CO_2	NO_x
MSG-Brenner			Ar	He	H_2	N_2	CO_2	NO_x
Wurzelschutz	10	Argon	Ar 100	He	H_2	N_2	CO_2	NO_x
Plasma			Ar	He	H_2	N_2	CO_2	NO_x
Pulver					**Schütthöhe**			
Typ					**Charge**			

Nahtvorbereitung

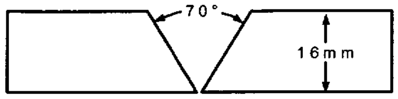

Nahtaufbau

Siehe beigefügte Zeichnung:

Oliver Brauckmann () / 17.11.2011

Schweißer / Datum

Grundwerkstoff:	Nicrofer 3220 H	Schweißzusatzwerkstoff:	S 7020 So 3	Ø 1,2 mm
Charge:	156122	Charge:	126161	
Werkstoffnummer:	1.4948	Werkstoffnummer:	2.48066	
Gas:	AW 2	FA:	103442167	
Länge:	500 mm	Prüfdatum:	13.05.2011	

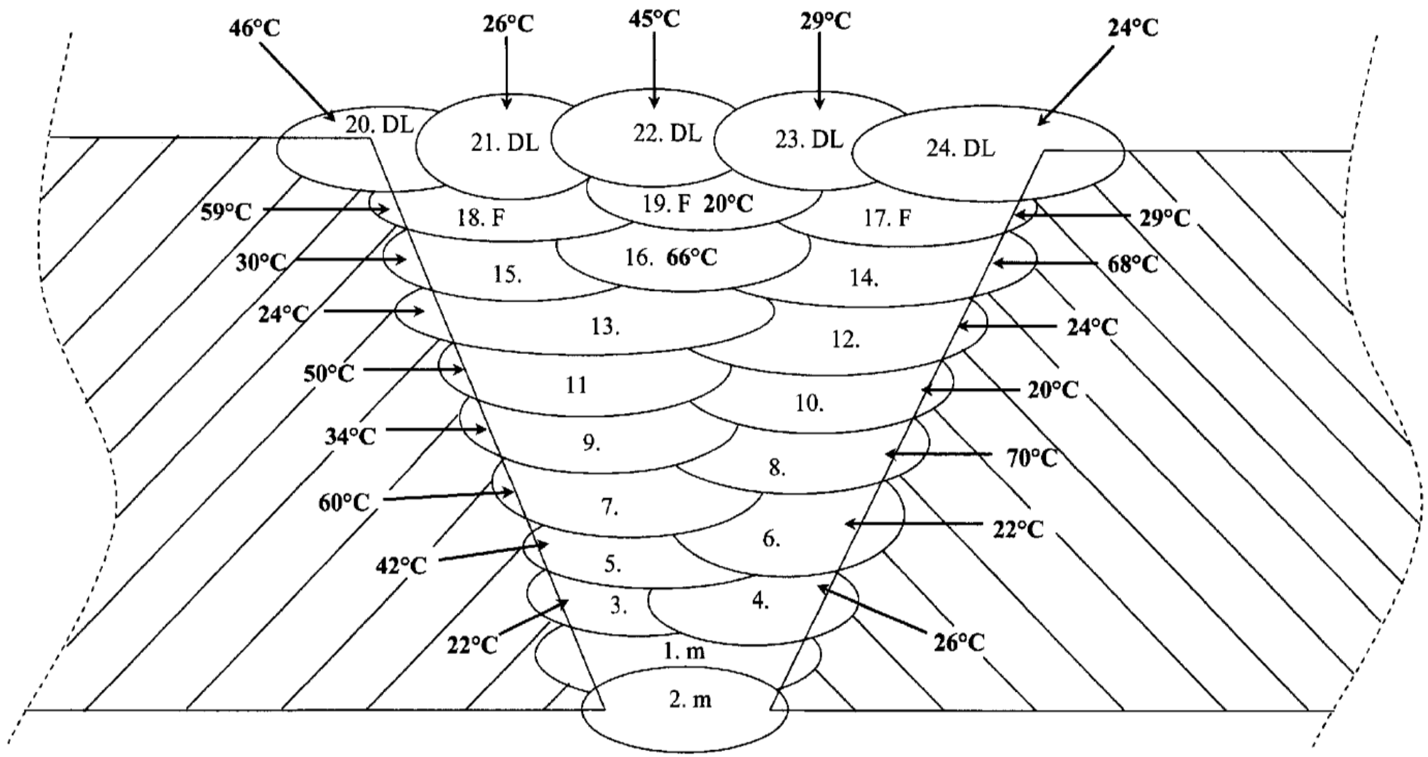

Ein Unternehmen von ThyssenKrupp Steel **ThyssenKrupp VDM** ThyssenKrupp VDM GmbH Produktbereich Blech

effstraße 23, D-58762 Altena Tel. +49 2392 552082
Postfach 1251, D-58742 Altena Fax +49 2392 552047
EMail KSawinski@TKS-VDM.THYSSENKRUPP.COM

Zertifikat EN 10204 **Nr. 31191/0** 3.2 C

Seite 1 von 1
gedruckt: 29.12.2004

ThyssenKrupp

Auftragsnr. 2329 | Lieferschein | Handelsmarke **NICROFER 3220 H 1.4958** | Herstellerzeichen VDM

Produkt
Musterblech, warmgewalzt, lösungsgeglüht, beidseitig geschliffen, geschnitten

Spezifikation	Werkstoff
ASTM B 409-01	UNS N08810
DIN 17460 09/92	X5NiCrAlTi 31 20
SEW 470-76	X 5 NiCrAlTi 32-20
VDTÜVBL. 434/03.99	X5NiCrAlTi 31 20

ThyssenKrupp VDM

Kleffstr. 23
- 58762 Altena

Pos.	Stück	Gew [kg]	Dimension [mm]	Charge	Los	
8	63		16,000x 150,0x 500,0	156122	103258397	Probe-Nr. 793

Analyse (Gew %)

Charge	Erschmelzung	C	S	Cr	Ni	Mn	Si	Ti	Nb	Cu	Fe	P	Al	Co
156122	EO/VD	0,06	<0,002	20,5	30,5	0,7	0,50	0,34	0,01	0,10	R46,7	0,010	0,27	0,1

Stückanalyse (Gew-%)

Charge	Los	Probe-Nr.	C	S	Cr	Ni	Mn	Si	Ti	Cu	P	Al	Co
156122	103258397	793-F	0,07	<0,002	20,5	30,5	0,7	0,51	0,35	0,10	0,010	0,28	0,1

Probenzustand: lösungsgeglüht
Zugversuch: 1 EN 10002-1 / Querprobe
Korngrösse: 1 EN 103

Los	Probe-Nr.		Temp [°C]	Rp0.2 [MPa]	Rp1.0 [MPa]	Rm [MPa]	Dehnung A [%]	A [%]	Z [%]	Korngrösse	Rekrist. [%]
103258397	793-F	1	RT	227	259	534	5	53 50	64		
103258397	793-1									1 Nr 2.5	100

Spektralanalytische Verwechslungsprüfung wurde durchgeführt: ohne Beanstandung
Dimensions- und visuelle Kontrolle durchgeführt: ohne Beanstandung
Kontrolliert: 63 Bleche 16 x 150 x 500 mm
Markierung: 1.4958 - 793

TÜ 4

Der Sachverständige des TÜV

LRQA Approval
Number 912097

Wir bestätigen hiermit, dass das oben aufgeführte Material in Übereinstimmung mit den Lieferspezifikationen des Auftrags ist.

Klaus Sawinski, Werkssachverständiger

Zeichen des Sachverständigen
Q

Dieses beglaubigte Prüfzeugnis darf nicht außer in Gänze ohne schriftliche Erlaubnis der herausgebenden Organisation reproduziert werden. Die Eintragung von falschen, fiktiven oder betrügerischen Angaben auf dem Zertifikat kann als Straftat nach Bundesgesetz bestraft werden.

ThyssenKrupp VDM

ThyssenKrupp

Produktbereich Draht · Service-Center

· Service Center
Postfach 16 40 · 58776 Werdohl

ThyssenKrupp VDM GmbH
Werk Altena
Kleffstr. 23

D -58762 Altena

Bestell-Nr.:	Musterbestellung Herr Kemper
VDM-Auftrags-Nr.:	7600400845
Pos.:	1
Lieferschein-Nr.:	8681624694
Pos.:	1
Zeugnis-Nr.:	74311 / 0
Datum:	21.10.2011

Abnahmeprüfzeugnis DIN EN 10204/01.05 3.1

Artikel-Nr.	Werkstoff	Produkt/Lieferzustand/Aufmachung
40174156 /51920010	NICROFER S 7020 S03 2.4806 NICR20MN3NB Ni 6082	SCHWEISSZUSATZ Runddraht gereinigt, blank, nachgezogen, gezogen SD 300 SCHWARZ
Abmessung (mm)	W.-NR. 2.4806	Liefervorschrift
1,200	ERNICR-3	DIN EN ISO 544 ANSI/AWS A5.14/A5.14M:2005 / 22.03.2005

Schmelzanalyse

Charge	C	S	N	Cr	Ni	Mn	Si	Ti	Nb	Cu	Fe
126161	0,003	0,002	0,025	20,4	R72,9	3,2	0,11	0,32	2,7	0,01	0,2
Charge	P	Mg	Co	Ta							
126161	0,002	0,002	<0,01	0,01							

Mechanische/Physikalische Eigenschaften

Charge	FA-Nr.	Rp0.2 (N/mm²) min	Rp0.2 (N/mm²) max	Rm (N/mm²) min	Rm (N/mm²) max	Bruchdehnung lo =100 mm min	Bruchdehnung lo =100 mm max	Gewicht (kg)	Anzahl
126161	103442167	1042	1042	1121	1121	7	7	30,1	2

Abnahmebeauftragter: Eva Petersmann
Tel: +49 2392 55-2635
Fax: +49 2392 55-2636
EMail: eva.petersmann@thyssenkrupp.com
Dieses Zeugnis wurde maschinell erstellt und ist ohne Unterschrift gültig

ThyssenKrupp VDM GmbH
Produktbereich Draht · Service Center
Goethestr. 59, 58791 Werdohl
Postfach 1640, 58776 Werdohl
Telefon: (02392) 55-4115, Telefax: (02392) 55-4121
Internet: www.thyssenkruppvdm.de

Vorsitzender des Aufsichtsrats: Clemens Iller
Geschäftsführung: Dr. Jürgen Olbrich,
Dipl.-Wirtsch.-Ing. Gerald Priegnitz, Dr.-Ing. Franz-Josef Wahlers
Handelsregister: Amtsgericht Altena / Westf. HRB 606
Sitz der Gesellschaft: Werdohl

KRUPP VDM

V D M
Werk Altena
Schweißlabor
z.Hd.Herrn Hoffmann

58762 Altena

Besteller/Bestell-Nr./vom Purchaser/Order No./of	Unsere Zeichen/Bearbeiter Responsible	Telefon-Durchwahl Direct Line	Datum Date
	TQB-Hu/mo	(02392) 55- 2618	07.02.1994

Abnahmeprüfzeugnis B / Inspection certificate B nach / according to EN 10204-3.1 B

Unsere Auftrags-Nr. Our Order No.	Prüf-Nr. Test No.	Erzeugnisform Product	Lieferzustand Condition of Delivery
945410-006 L-Nr. 5249		Stäbe	blank, nachgezogen

Werkstoff Quality	Werkstoff-Nr. Material No.	Erschmelz. Art Melting Process	Lieferbedingungen und/oder amtliche Vorschriften Terms of Delivery and/or Official Regulations
Nicrofer S 7020	2.4806	E	

Pos. Item	Probe Nr. No. of Sample	Anzahl Quantity	Abmessungen Dimensions	0,2% Dehngr. Yield Strength MPa	Zugfestigkeit Tensile Strength MPa	Bruchdehng. Elongation L_0 =	Gewicht Weight
			2,50 mm x 1000 mm				75,-- kg

Probe Nr. No. of Sample	Charge Cast	C	Cr	Ni	Mn	Si	Mo	Fe	Ti/~~Nb~~	Cu
	380367	0,012	20,80	72,10	3,13	0,08		0,77	0,25	0,01

Chemische Zusammensetzung % (Schmelzanalyse) / Chemical Composition % (of Cast)

Nb+Ta	S	Co
2,700	0,003	0,01

Krupp VDM GmbH
Der Werkssachverständige/Works inspector

8/2.94

Zeichen des Herstellers
Mark of the Manufacturer

N 1419 93-05

Krupp VDM GmbH, Postfach 18 20, D-58778 Werdohl, Plettenberger Straße 2, Telefon (0 23 92) 55-0, Telex 8 26 433-0 vm d, Fax (0 23 92) 55-22 17

Appendix B

B.1 Single specimen data of all the tensile tests

Specimen Number	Irr. experiment	Base/Weld and Direction: RD/TD	Test temperature (°C)	0.2% offset yield stress (MPa)	0.5% offset yield stress (MPa)	1.0% offset yield stress (MPa)	2.0% offset yield stress (MPa)	5.0% offset yield stress (MPa)	10% offset yield stress (MPa)	20% offset yield stress (MPa)	Tensile strength (MPa)	Total Elongation (%)	Uniform Plastic Elongation (%)	Reduction of area (%) (measured on specimen)	Strain rate (s^{-1})
P345	un-irradiated	Base TD	RT	202	228	248	271	318	377	468	547	52.7	41.1	68	5.00E-04
P346	un-irradiated	Base TD	700	123	139	149	167	207	257	320	333	46.5	27.9	56.1	5.00E-04
P344	un-irradiated	Base TD	800	116	132	147	170	180	174	161	180	84.8	3.6	78.4	5.00E-04
P405	un-irradiated	Base RD	RT	223	238	254	275	319	380	474	550	49.6	39.4	58.3	5.00E-04
P406	un-irradiated	Base RD	700	139	157	174	196	239	284	304	306	44.8	18.3	62.3	5.00E-04
P407	un-irradiated	Base RD	800	118	130	145	166	177	171	159	178	73.5	4.1	73.1	5.00E-04
P397	un-irradiated	Weld RD	RT	439	468	489	510	545	584	586	614	25.8	16.7	64	5.00E-04
P398	un-irradiated	Weld RD	700	303	321	339	359	384	365	_	387	17.1	6.7	42.2	5.00E-04
P399	un-irradiated	Weld RD	800	247	249	249	244	235	215	3	251	20.3	0.4	63.5	5.00E-04

B.2 Single specimen data of all LCF tests

Specimen Number	Material	Irradiation Dose (dpa)	Test Temp (°C)	Strain range (%)	Holdtime Tens (sec)	Holdtime Comp (sec)	Nr Cycles to 50% reduction (N50=Nf)	Max Stress Cycle 1 (MPa)	Max Stress Cycle 5 (MPa)	Max Stress Cycle 10 (MPa)	Max Stress Cycle 100 (MPa)	Min Stress Cycle 1 (MPa)	Min Stress Cycle 5 (MPa)	Min Stress Cycle 10 (MPa)	Min Stress Cycle 100 (MPa)	(Stress Ampl)/2 Cycle 1 (MPa)	(Stress Ampl)/2 Cycle 5 (MPa)	(Stress Ampl)/2 Cycle 10 (MPa)	(Stress Ampl)/2 Cycle 100 (MPa)	Peak Stress Ampl(MPa)	Nr Cycles to peak sat	Pl. strain range at peak Sa(%)	Saturation (Stress Ampl)/2(MPa)	Pl. strain range at sat (%)	El. strain range at sat (%)	Tot. strain range at sat (%)	N25
P419	Alloy 800H	0	800	0,60	0	0	1576	127,14	150,72	153,97	153,75	132,78	144,79	148,01	150,03	129,96	147,76	150,99	151,89	154,25	616	0,36	152,86	0,37	0,23	0,60	1498
P417	Alloy 800H	0	800	0,90	0	0	735	130,78	166,22	167,23	168,79	138,35	161,81	162,82	165,89	134,56	164,02	165,03	167,34	167,62	200	0,64	161,96	0,63	0,26	0,89	710
P423	Alloy 800H	0	800	1,20	0	0	309	158,03	187,85	187,81	183,86	164,18	184,00	183,19	181,96	161,11	185,92	185,50	182,91	186,21	8	0,87	179,74	0,87	0,31	1,18	277
Tes1	Alloy 800H	0	800	1,50	0	0	372	166,95	198,54	198,13	190,12	171,17	194,04	193,51	182,97	169,06	196,29	195,82	186,54	197,06	6	1,21	182,15	1,19	0,31	1,50	339
Tes4	Alloy 800H	0	800	0,60	1000	0	323	130,47	148,87	147,41	148,56	140,41	148,28	148,84	153,30	135,44	148,58	148,13	150,93	150,93	100	0,46	148,08	0,45	0,16	0,61	285
Te3b	Alloy 800H	0	800	0,9	1000	0	195	143,42	174,84	174,66	164,64	158,54	171,855	172,865	169,402	150,98	173,35	173,8	167	174,25	20	0,74	167,4	0,752	0,1594	0,9116	180
Tes2	Alloy 800H	0	800	1,20	1000	0	125	141,82	174,15	172,59	156,84	163,91	175,43	178,44	175,10	152,86	174,79	175,52	165,97	180,61	35	0,95	175,95	0,96	0,25	1,21	123
P424	Alloy 800H	0	800	1,50	1000	0	171	167,84	189,58	189,60	164,95	177,21	185,30	184,88	168,44	172,53	187,44	187,24	166,69	188,12	9	1,30	171,11	1,28	0,22	1,50	143

Appendix C

C.1 EDS results precipitate analyses of Base Material

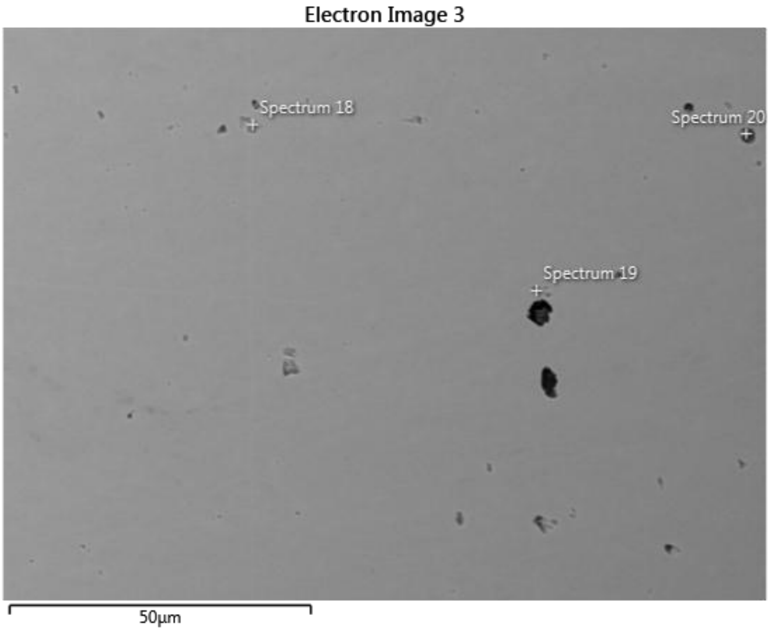

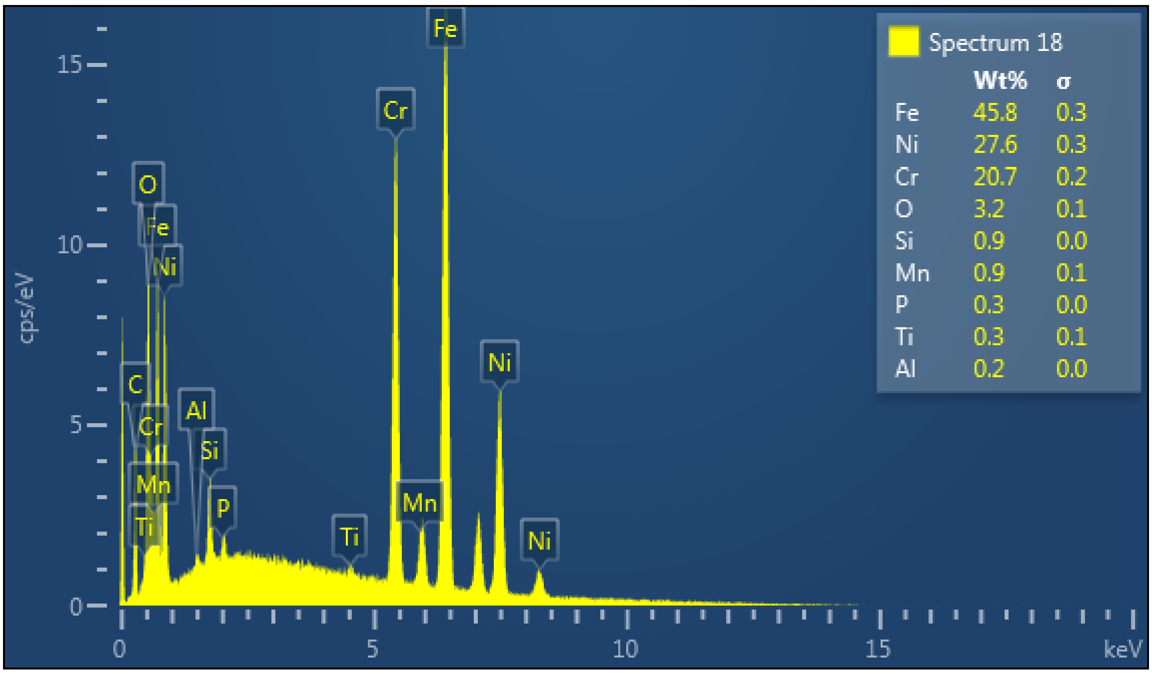

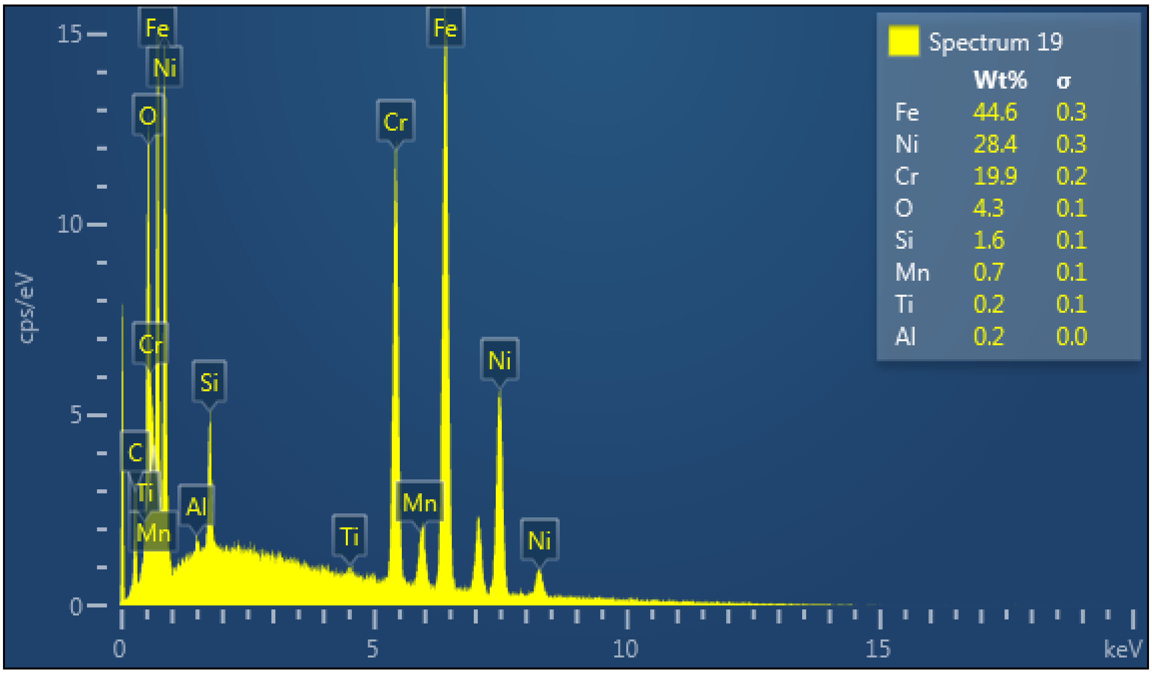
Spectrum 19
Wt% σ
Fe 44.6 0.3
Ni 28.4 0.3
Cr 19.9 0.2
O 4.3 0.1
Si 1.6 0.1
Mn 0.7 0.1
Ti 0.2 0.1
Al 0.2 0.0
cps/eV
keV
Fe
Ni
O
Cr
C
Ti
Mn
Si
Al
Ti
Cr
Mn
Fe
Ni
Ni

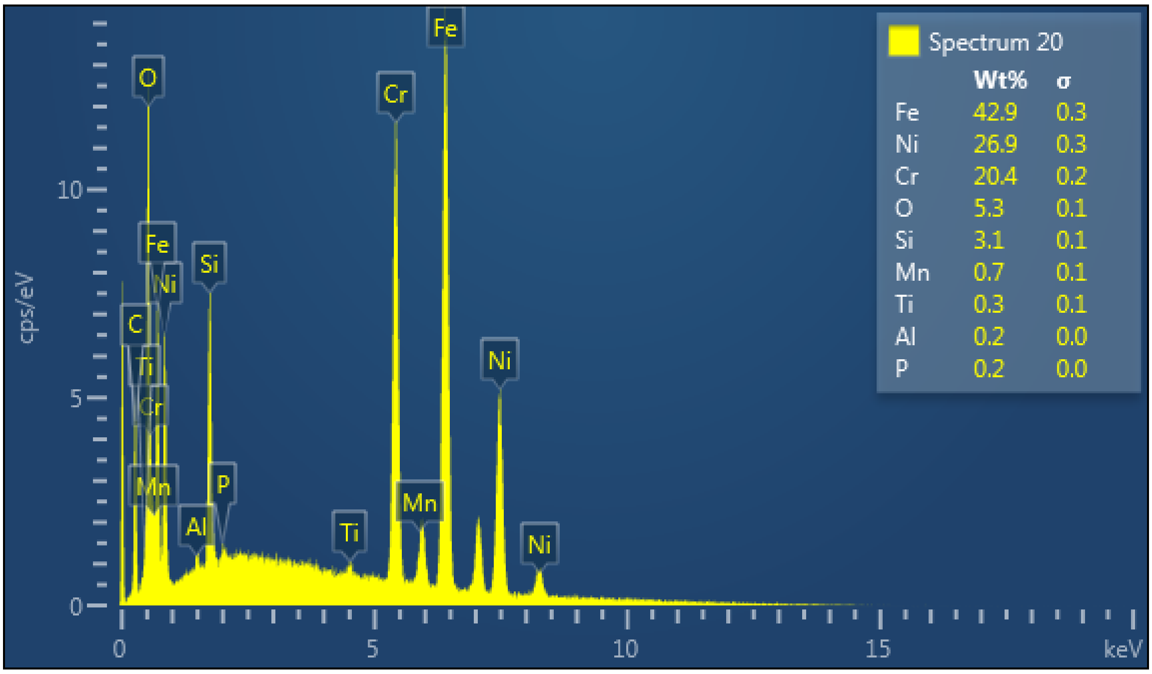
Spectrum 20
Wt% σ
Fe 42.9 0.3
Ni 26.9 0.3
Cr 20.4 0.2
O 5.3 0.1
Si 3.1 0.1
Mn 0.7 0.1
Ti 0.3 0.1
Al 0.2 0.0
P 0.2 0.0
cps/eV
keV
O
Fe
Ni
C
Ti
Cr
Mn
Si
P
Al
Ti
Cr
Mn
Fe
Ni
Ni

Electron Image 4

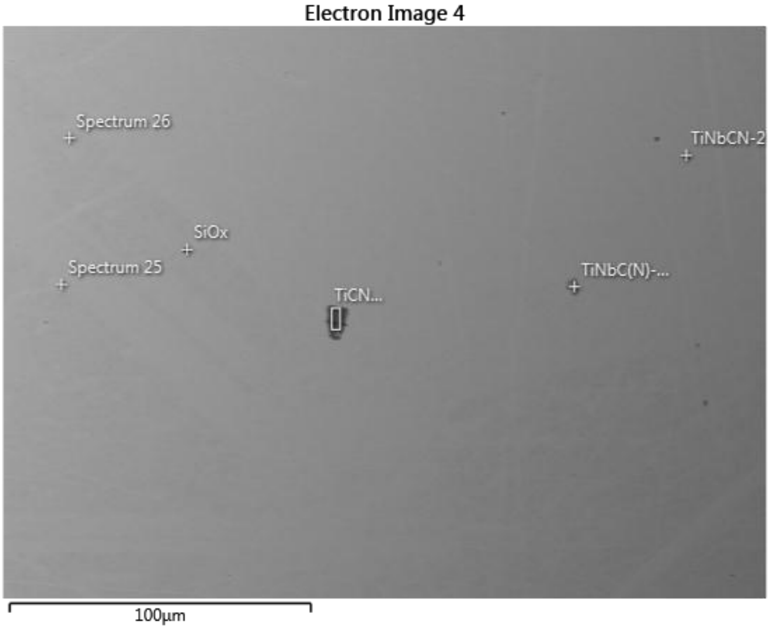

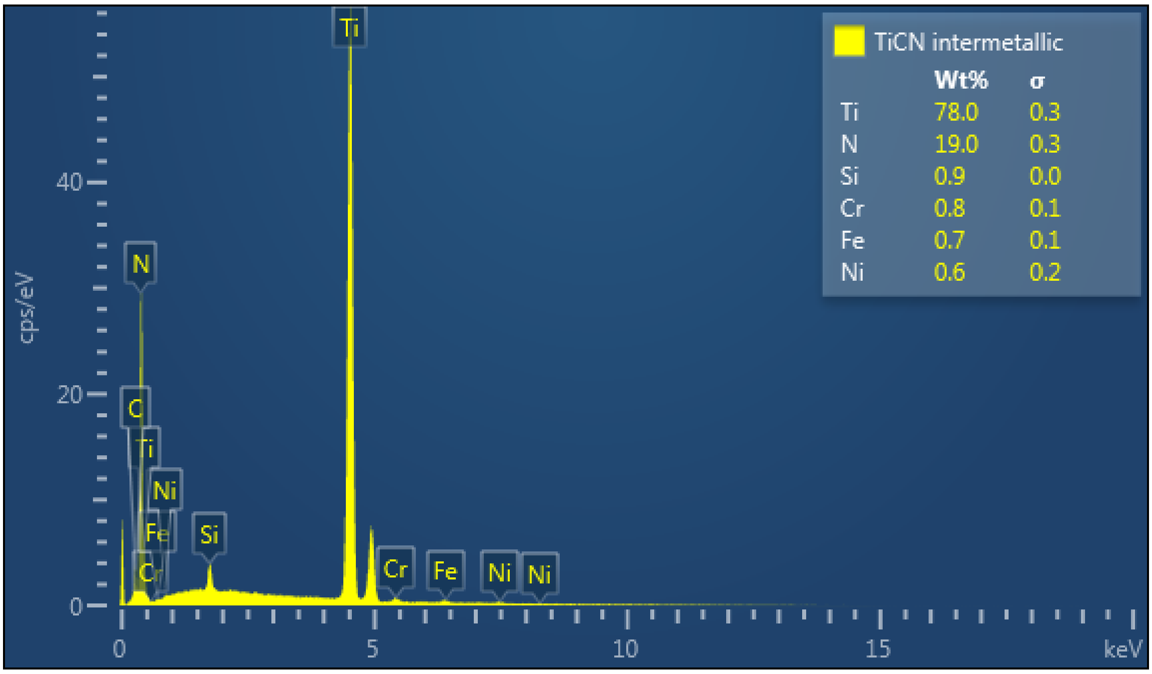

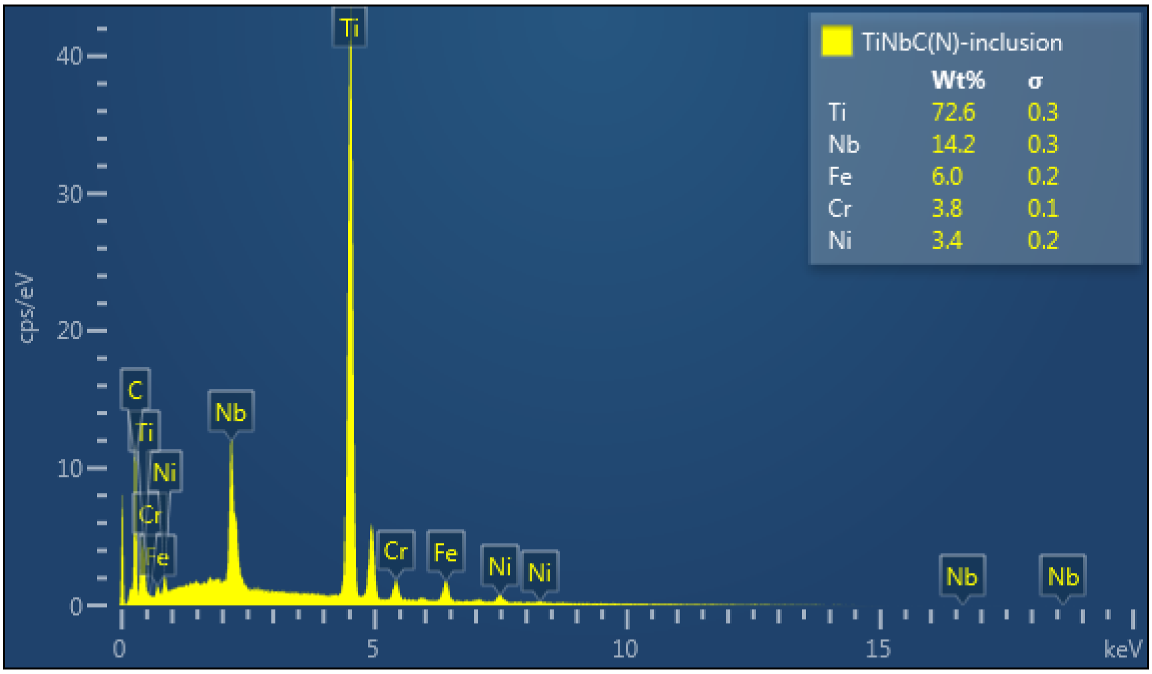
TiNbC(N)-inclusion
Wt% σ
Ti 72.6 0.3
Nb 14.2 0.3
Fe 6.0 0.2
Cr 3.8 0.1
Ni 3.4 0.2
cps/eV
keV

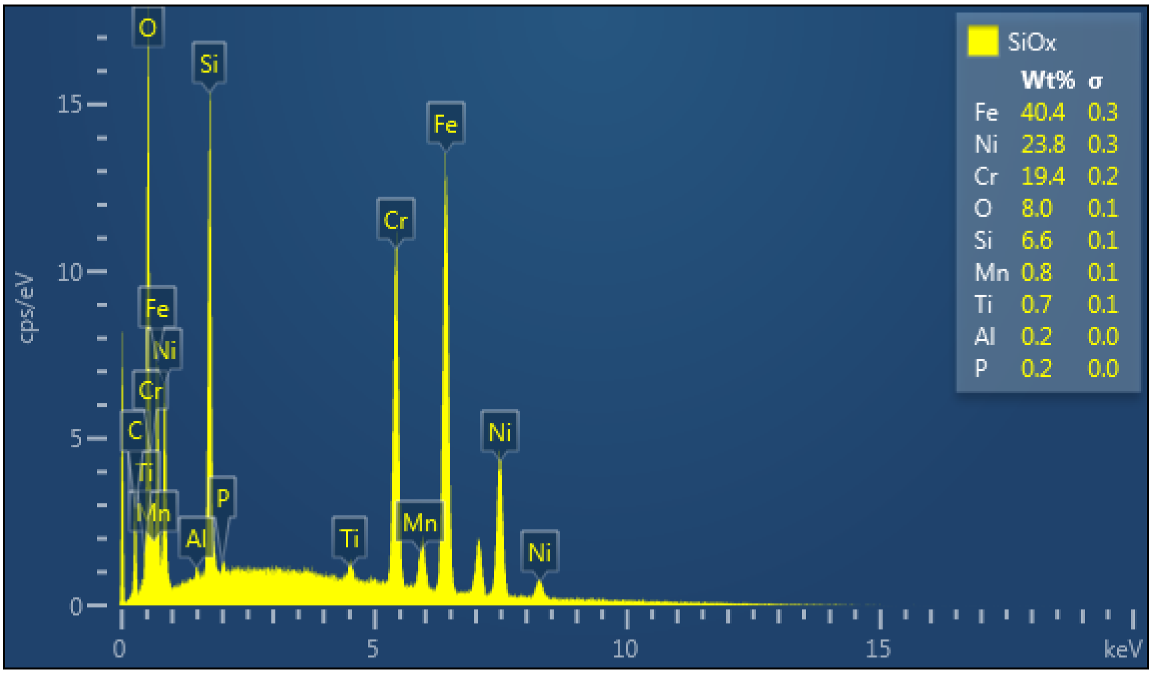
SiOx
Wt% σ
Fe 40.4 0.3
Ni 23.8 0.3
Cr 19.4 0.2
O 8.0 0.1
Si 6.6 0.1
Mn 0.8 0.1
Ti 0.7 0.1
Al 0.2 0.0
P 0.2 0.0
cps/eV
keV

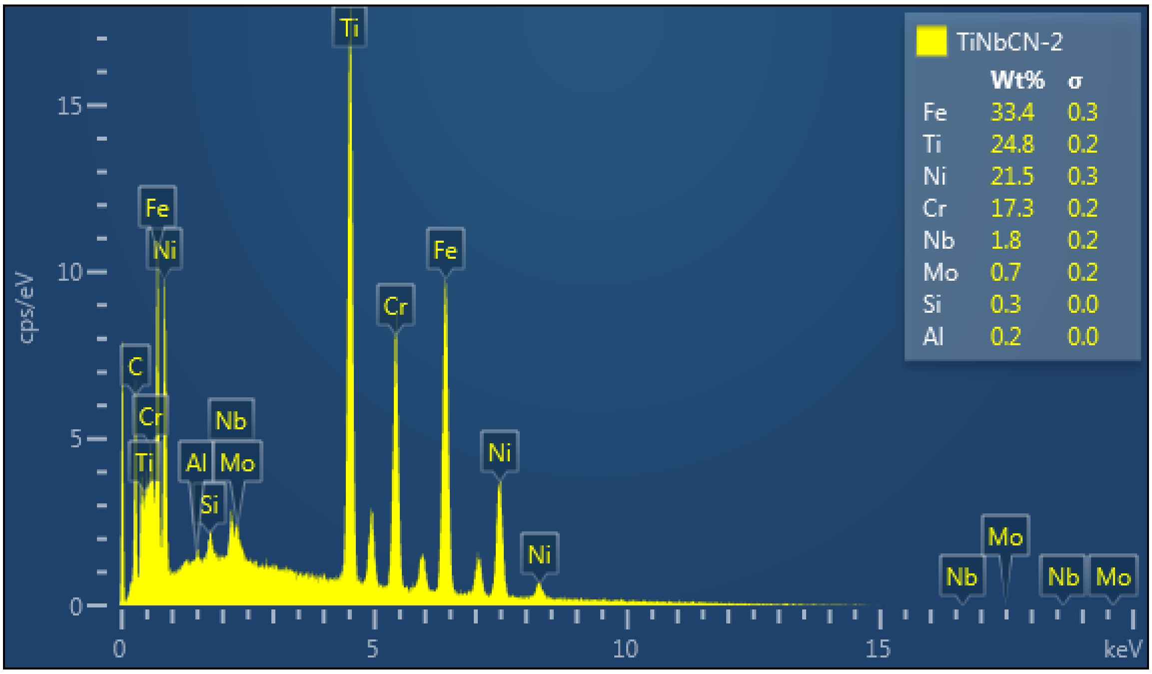
TiNbCN-2
Wt% σ
Fe 33.4 0.3
Ti 24.8 0.2
Ni 21.5 0.3
Cr 17.3 0.2
Nb 1.8 0.2
Mo 0.7 0.2
Si 0.3 0.0
Al 0.2 0.0
cps/eV
keV
Ti
Fe
Ni
Cr
C
Nb
Al
Mo
Si
0
5
10
15

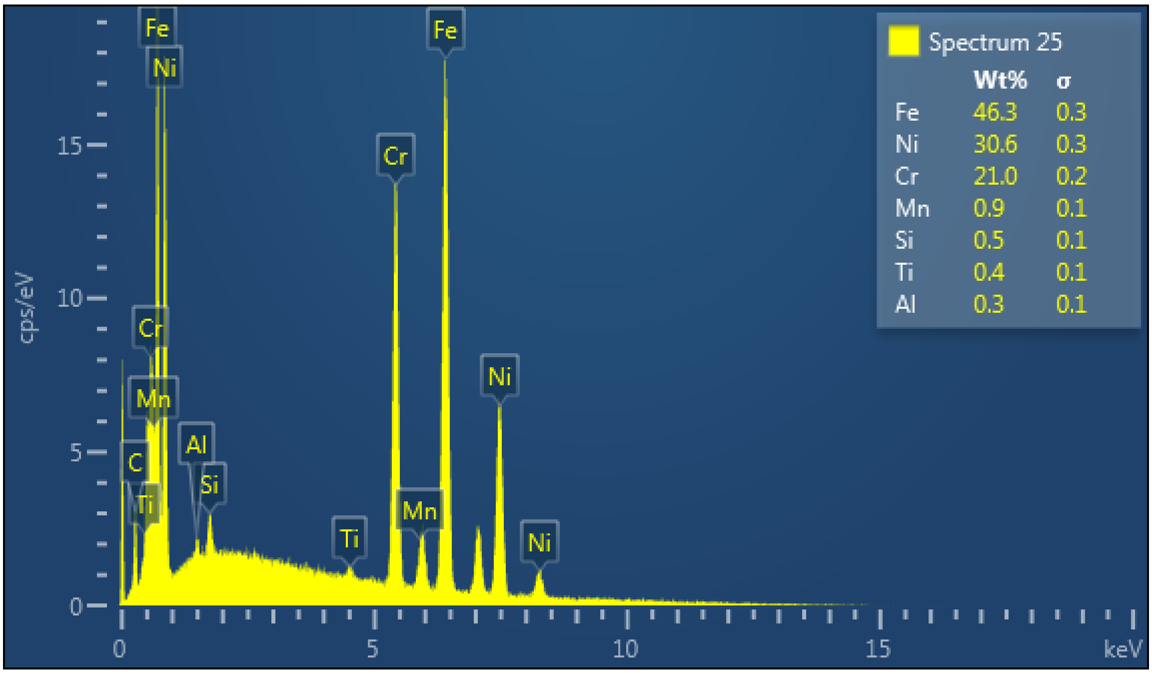
Spectrum 25
Wt% σ
Fe 46.3 0.3
Ni 30.6 0.3
Cr 21.0 0.2
Mn 0.9 0.1
Si 0.5 0.1
Ti 0.4 0.1
Al 0.3 0.1
cps/eV
keV
Fe
Ni
Cr
Mn
C
Ti
Al
Si
0
5
10
15

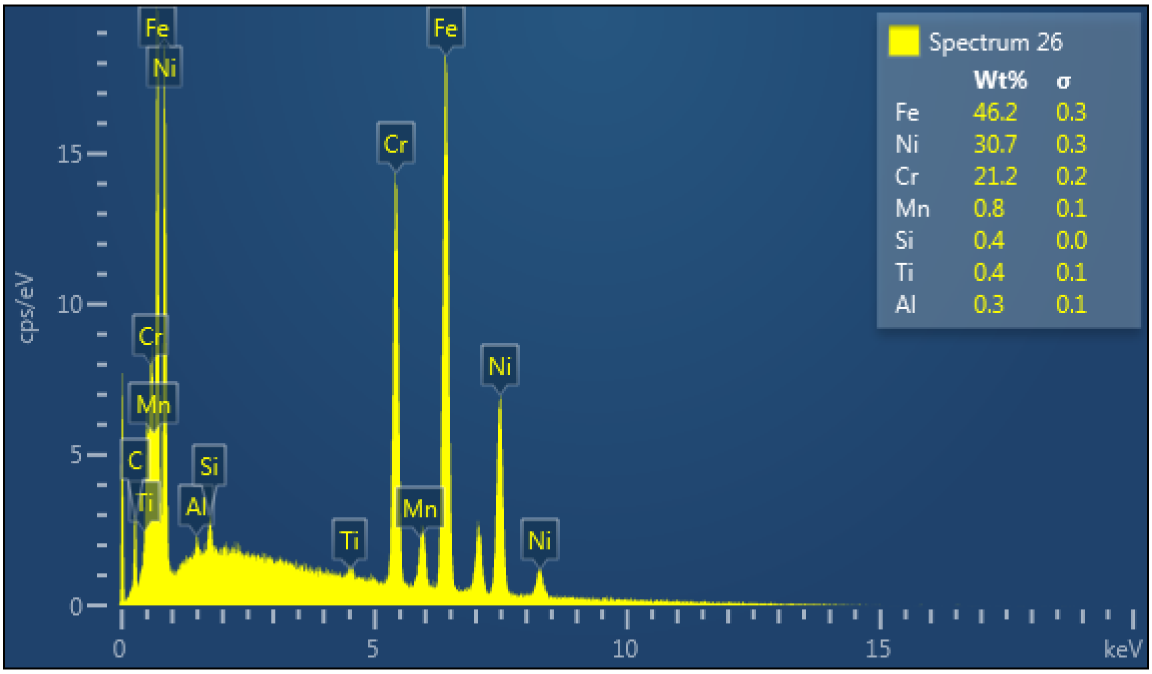
Fe
Ni
Fe
Cr
Cr
Mn
C
Ti
Si
Al
Ti
Mn
Ni
Ni
cps/eV
0
5
10
15
0
5
10
15
keV
Spectrum 26
Wt% σ
Fe 46.2 0.3
Ni 30.7 0.3
Cr 21.2 0.2
Mn 0.8 0.1
Si 0.4 0.0
Ti 0.4 0.1
Al 0.3 0.1

Electron Image 5

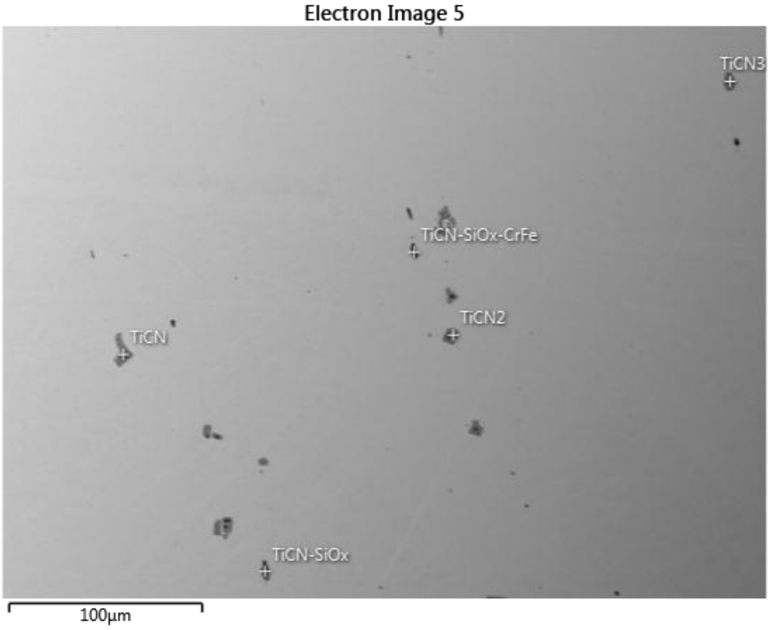

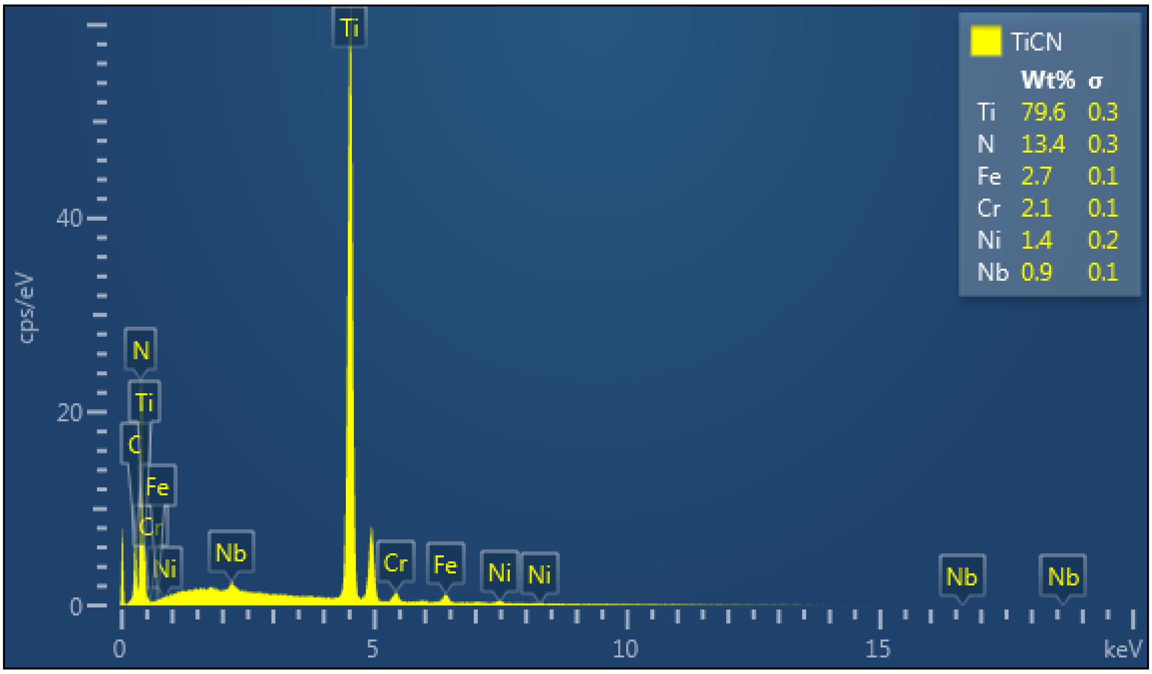

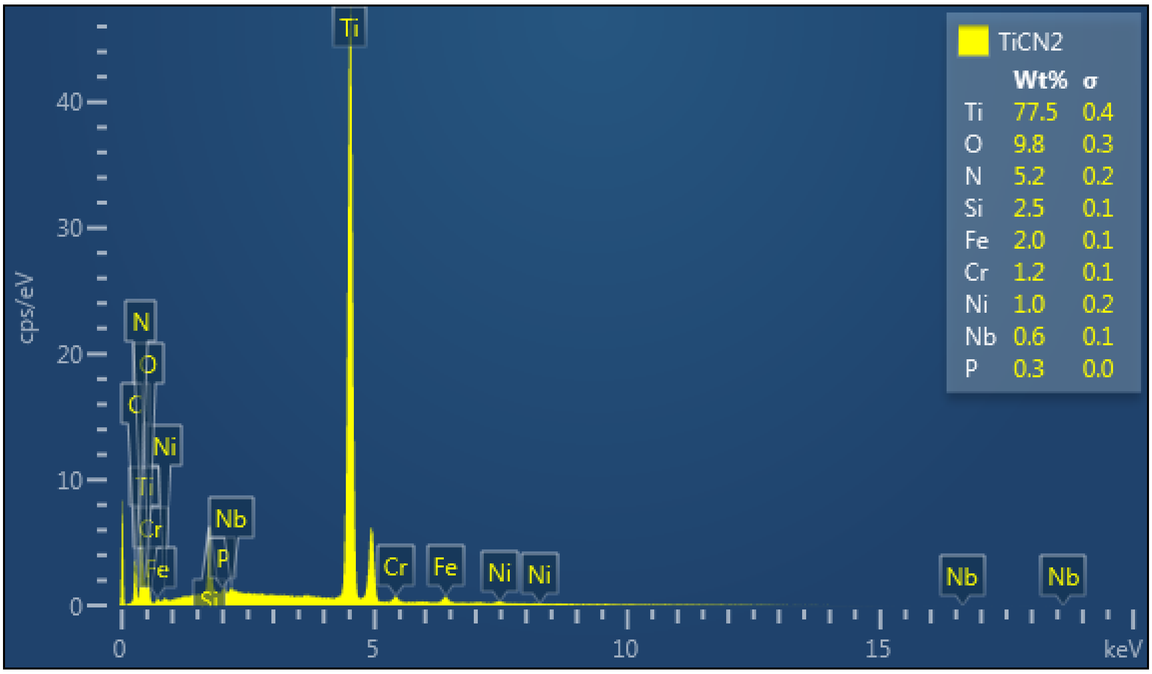
TiCN2
Wt% σ
Ti 77.5 0.4
O 9.8 0.3
N 5.2 0.2
Si 2.5 0.1
Fe 2.0 0.1
Cr 1.2 0.1
Ni 1.0 0.2
Nb 0.6 0.1
P 0.3 0.0
cps/eV
keV

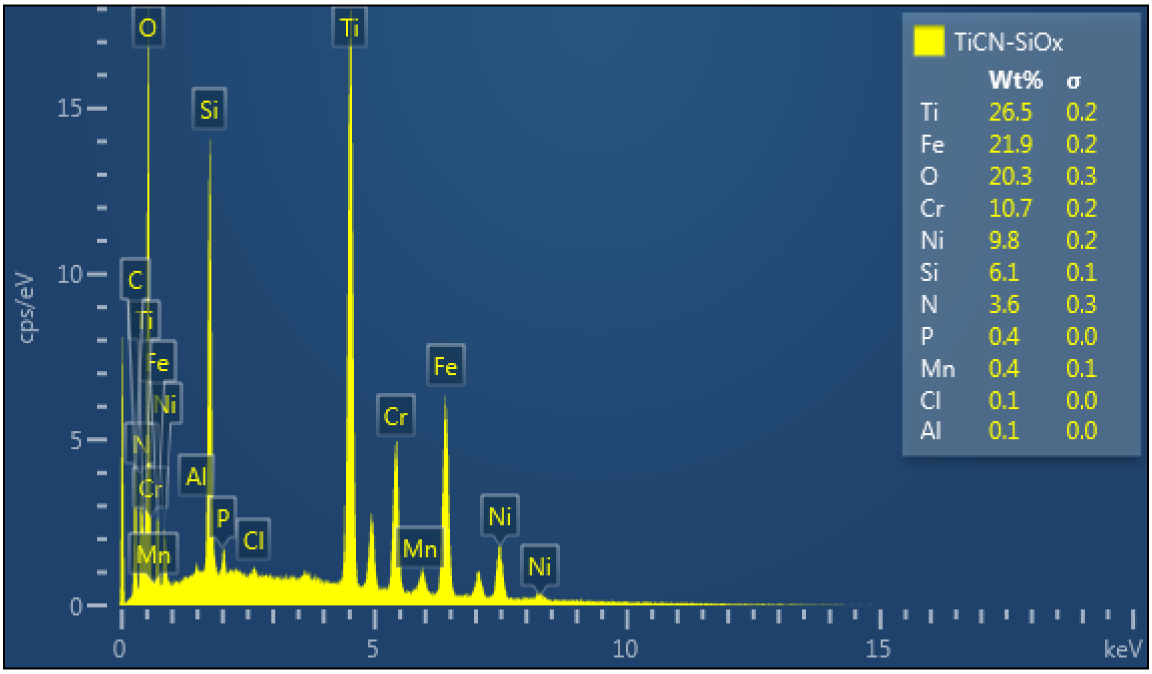
TiCN-SiOx
Wt% σ
Ti 26.5 0.2
Fe 21.9 0.2
O 20.3 0.3
Cr 10.7 0.2
Ni 9.8 0.2
Si 6.1 0.1
N 3.6 0.3
P 0.4 0.0
Mn 0.4 0.1
Cl 0.1 0.0
Al 0.1 0.0
cps/eV
keV

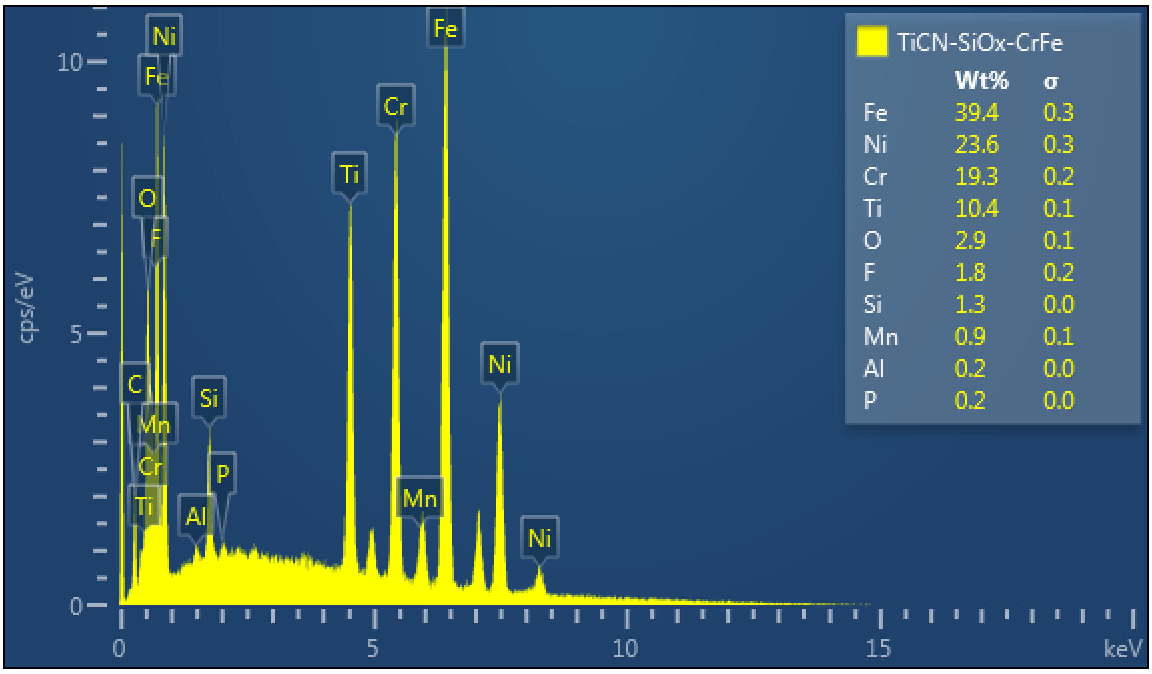
TiCN-SiOx-CrFe
Wt% σ
Fe 39.4 0.3
Ni 23.6 0.3
Cr 19.3 0.2
Ti 10.4 0.1
O 2.9 0.1
F 1.8 0.2
Si 1.3 0.0
Mn 0.9 0.1
Al 0.2 0.0
P 0.2 0.0
cps/eV
keV

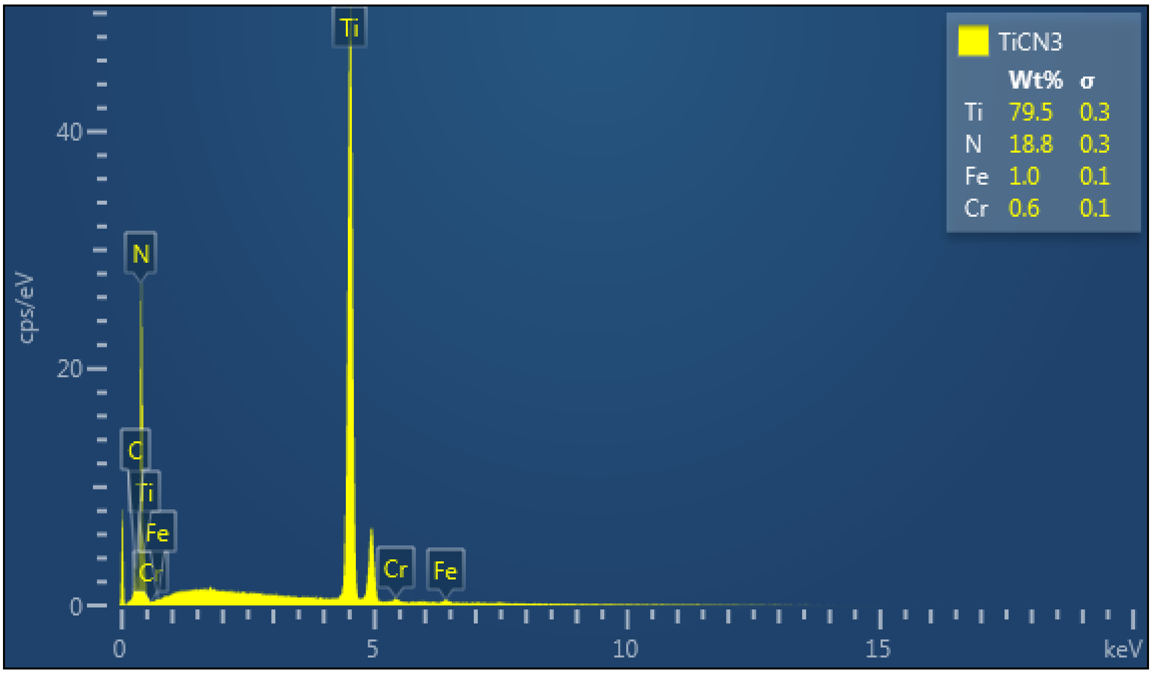
TiCN3
Wt% σ
Ti 79.5 0.3
N 18.8 0.3
Fe 1.0 0.1
Cr 0.6 0.1
cps/eV
keV

C.2 EDS results of weld material

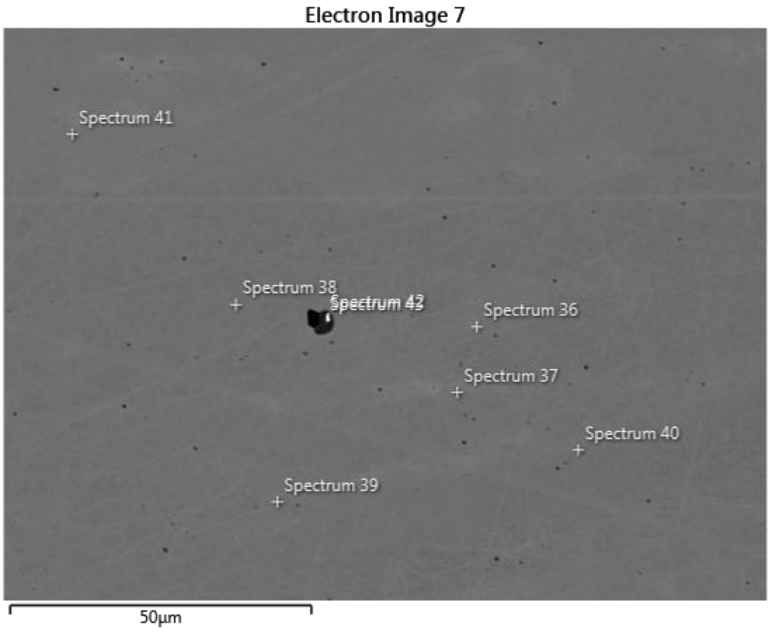

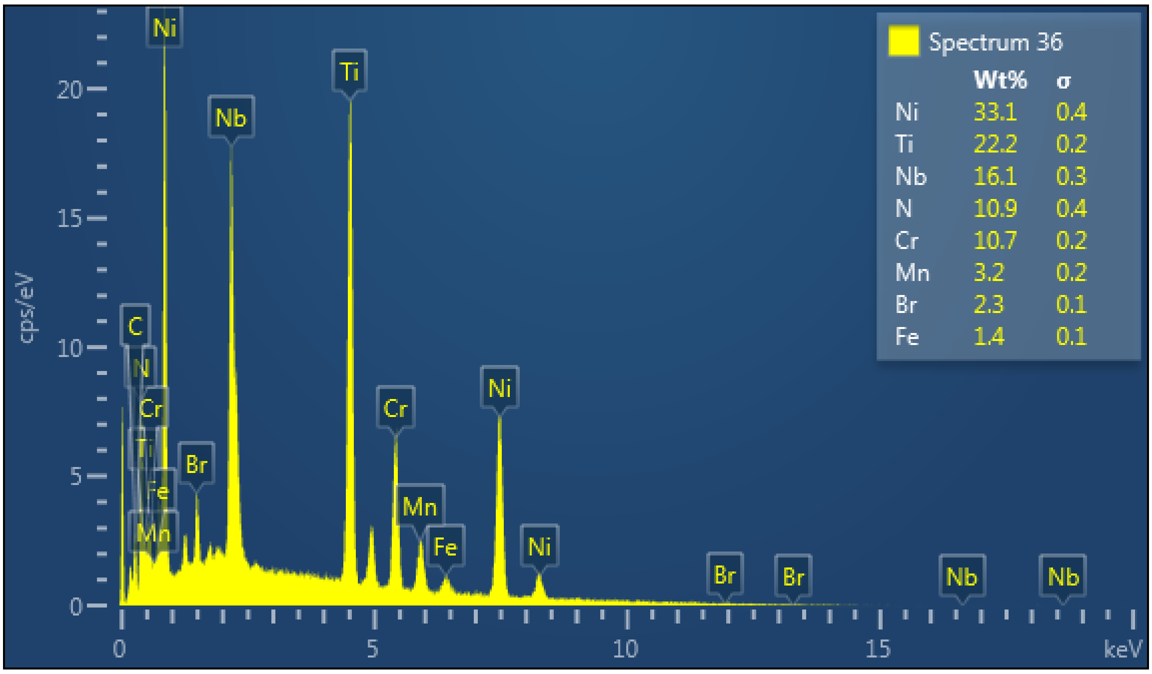

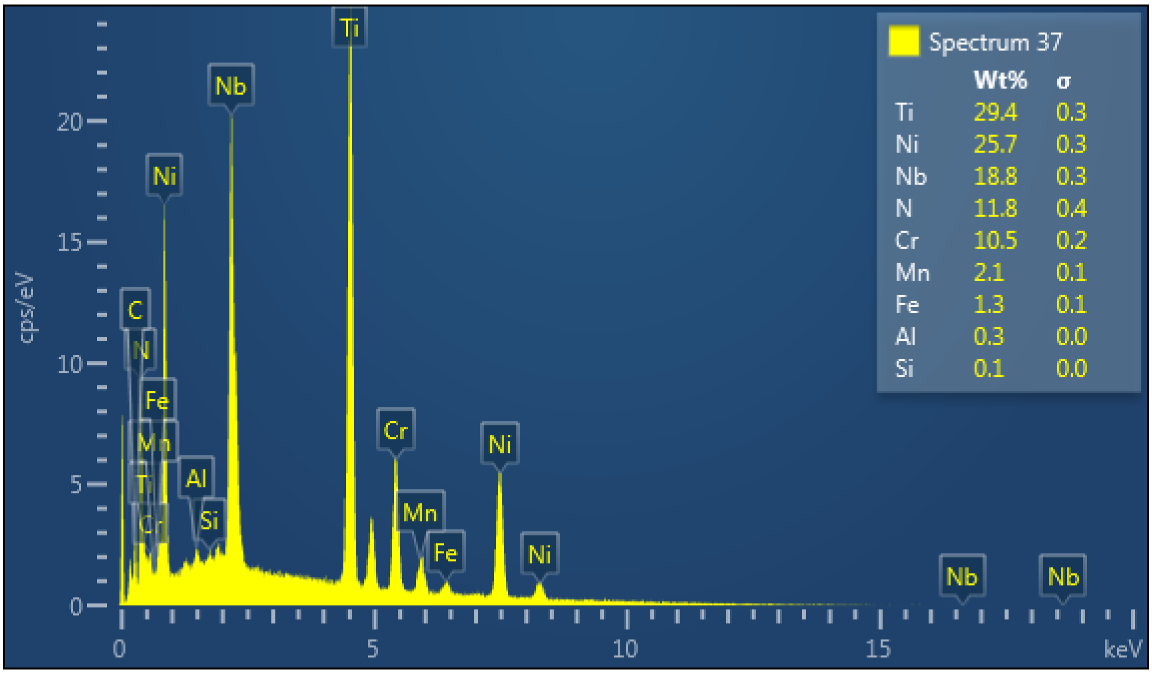
Spectrum 37
Wt% σ
Ti 29.4 0.3
Ni 25.7 0.3
Nb 18.8 0.3
N 11.8 0.4
Cr 10.5 0.2
Mn 2.1 0.1
Fe 1.3 0.1
Al 0.3 0.0
Si 0.1 0.0
cps/eV
keV
Ti
Nb
Ni
C
N
Fe
Mn
Al
Si
Cr
Ni
Mn
Fe
Ni
Nb
Nb

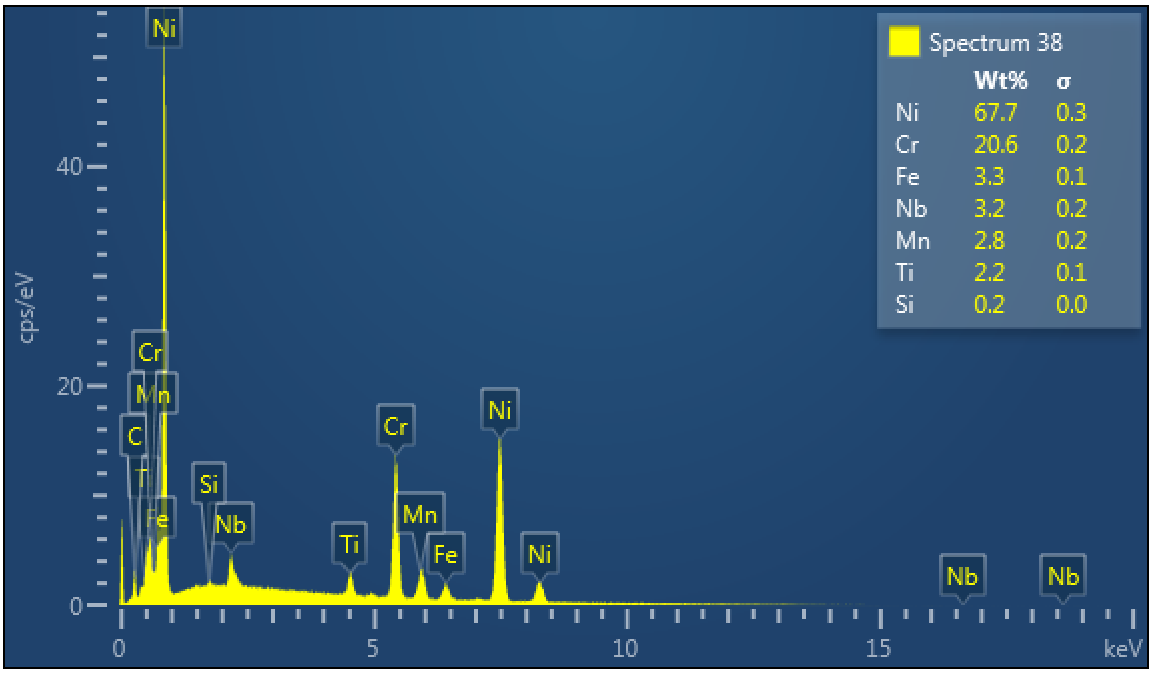
Spectrum 38
Wt% σ
Ni 67.7 0.3
Cr 20.6 0.2
Fe 3.3 0.1
Nb 3.2 0.2
Mn 2.8 0.2
Ti 2.2 0.1
Si 0.2 0.0
cps/eV
keV
Ni
Cr
Mn
C
Si
Nb
Fe
Ti
Cr
Ni
Mn
Fe
Ni
Nb
Nb

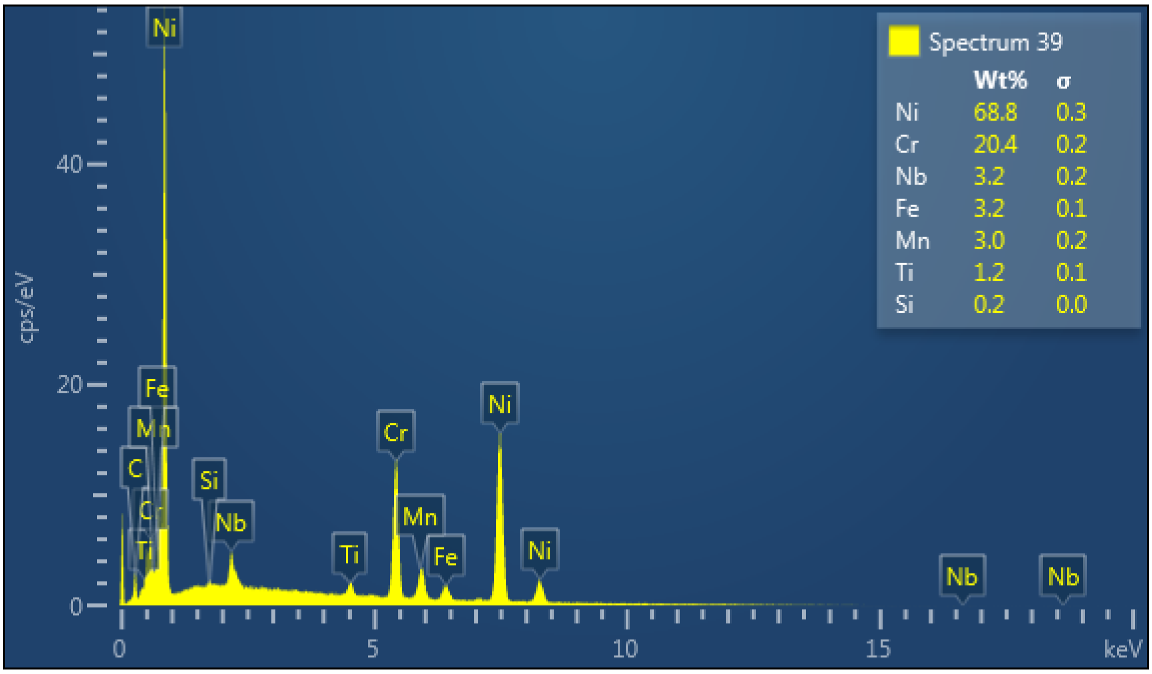

Spectrum 39
Wt% σ
Ni 68.8 0.3
Cr 20.4 0.2
Nb 3.2 0.2
Fe 3.2 0.1
Mn 3.0 0.2
Ti 1.2 0.1
Si 0.2 0.0
cps/eV
40
20
0
0
5
10
15
keV
Ni
Fe
Mn
C
Cr
Ti
Si
Nb
Ti
Cr
Mn
Fe
Ni
Ni
Nb
Nb

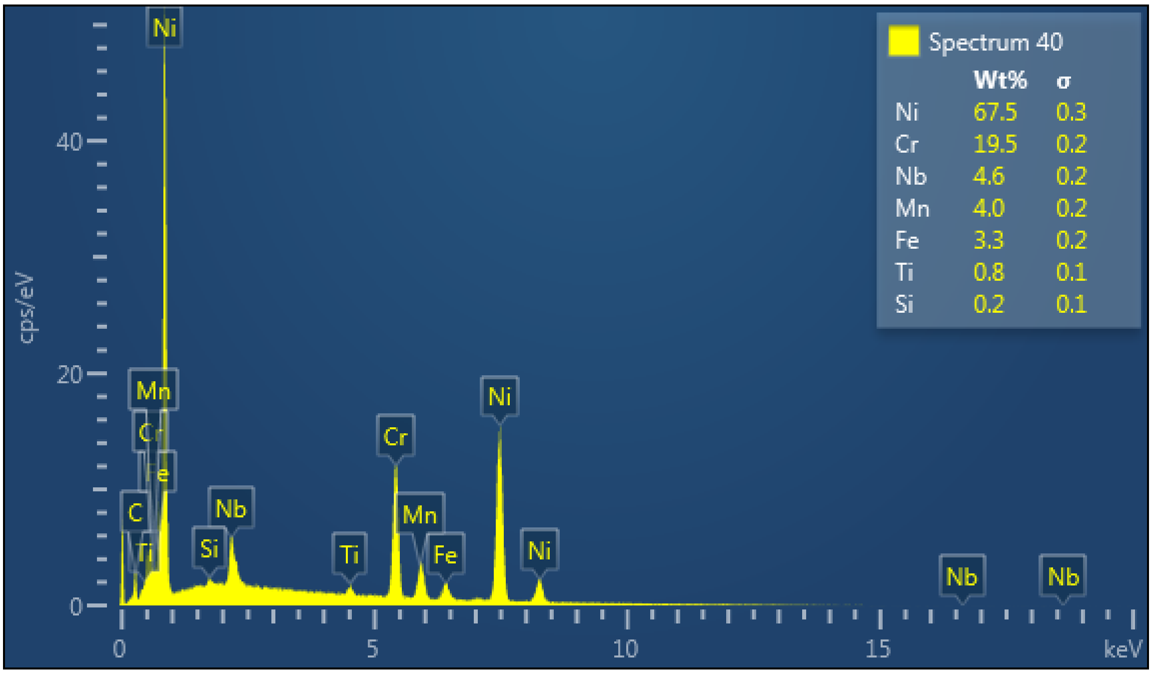

Spectrum 40
Wt% σ
Ni 67.5 0.3
Cr 19.5 0.2
Nb 4.6 0.2
Mn 4.0 0.2
Fe 3.3 0.2
Ti 0.8 0.1
Si 0.2 0.1
cps/eV
40
20
0
0
5
10
15
keV
Ni
Mn
Cr
Fe
C
Ti
Nb
Si
Ti
Cr
Mn
Fe
Ni
Ni
Nb
Nb

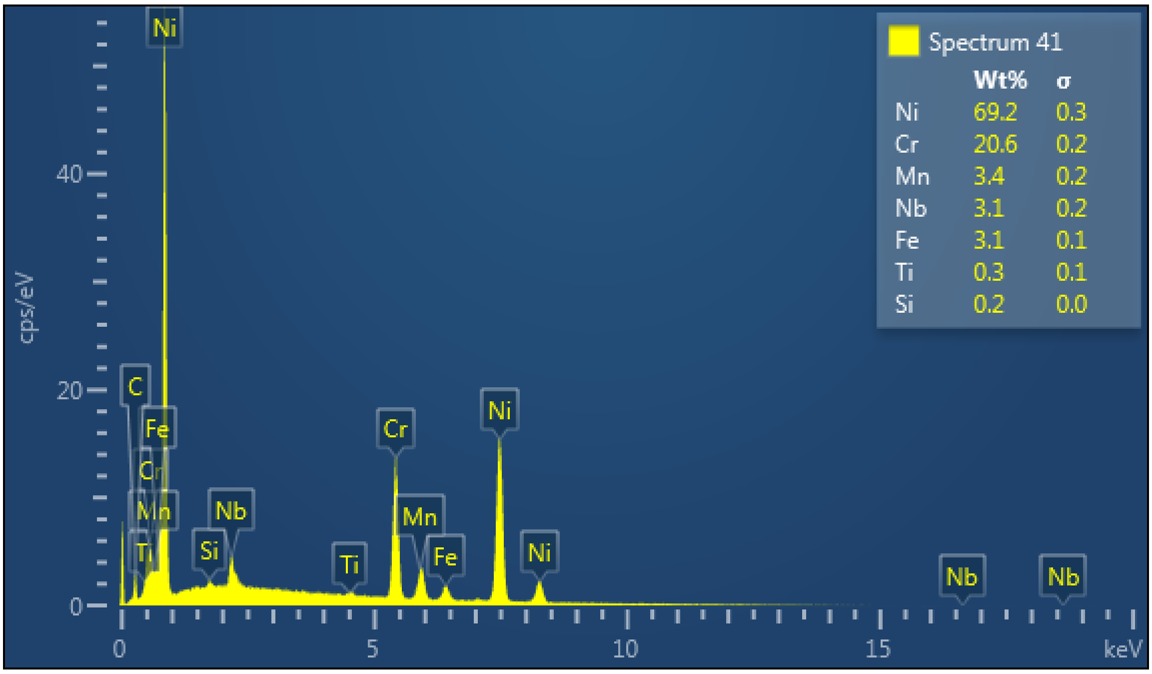
Spectrum 41
Wt% σ
Ni 69.2 0.3
Cr 20.6 0.2
Mn 3.4 0.2
Nb 3.1 0.2
Fe 3.1 0.1
Ti 0.3 0.1
Si 0.2 0.0
cps/eV
keV

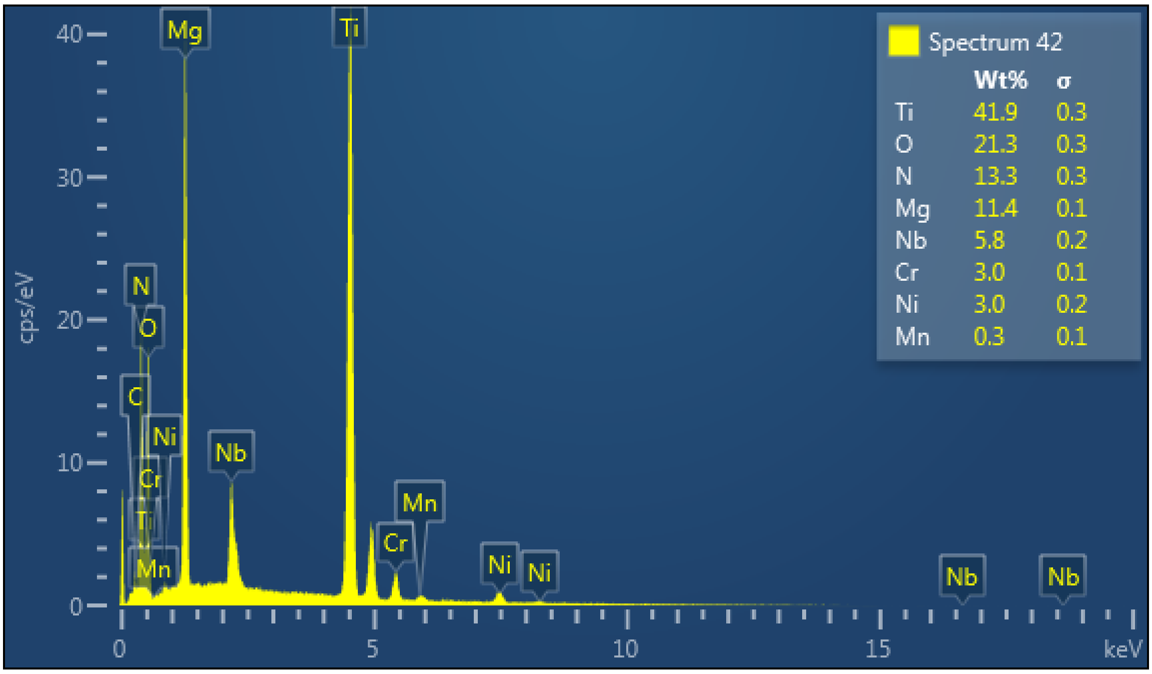
Spectrum 42
Wt% σ
Ti 41.9 0.3
O 21.3 0.3
N 13.3 0.3
Mg 11.4 0.1
Nb 5.8 0.2
Cr 3.0 0.1
Ni 3.0 0.2
Mn 0.3 0.1
cps/eV
keV

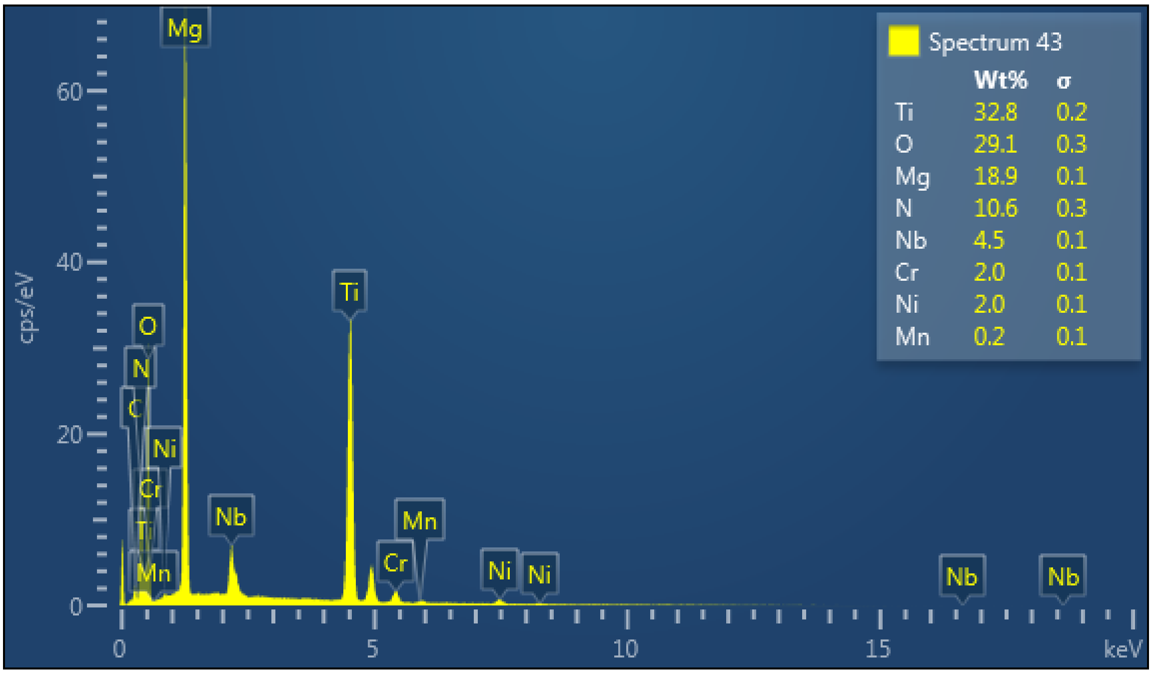
Spectrum 43
Wt% σ
Ti 32.8 0.2
O 29.1 0.3
Mg 18.9 0.1
N 10.6 0.3
Nb 4.5 0.1
Cr 2.0 0.1
Ni 2.0 0.1
Mn 0.2 0.1
cps/eV
keV